AQP4-negative and myelin-negative by definition). Patterns associated with focal necrosis or cavity formation were expressed as "Patterns X & N" (X = A, B, C or D).

RESULTS

Immunohistochemical findings in control brains

AQP4 and GFAP staining patterns as well as the deposition of immunoglobulins and activated complement in normal and diseased CNS tissues were described in detail in our previous report (33). Briefly, in normal cerebral tissues, AQP4 staining was more pronounced in the cortex than in the white matter, with staining emphasized in the perivascular foot processes. The glial limiting membranes and subependymal astrocytes also strongly expressed AQP4. By contrast, GFAP immunoreactivity was preferentially observed in the cerebral white matter while in the cortex, and except for the strong staining of the glial limiting membranes, only a few astrocytes were immunopositive for GFAP. Reactive astrocytes and gliotic scars were strongly immunopositive for both AQP4 and GFAP. In control cases, faint, diffuse IgG immunoreactivity in the neuronal soma, neuropil, oligodendrocytes, astrocytes, glial limiting membranes and ependymal epithelium was observed, but not in the white matter. IgM, C3d and C9neo immunoreactivities were generally confined to a small number of blood vessel walls and the perivascular regions, if any. Activated complement was not usually co-localized with immunoglobulins.

Immunohistochemical findings in NMO and NMO spectrum disorders

Preferential loss or decrease of AQP4 immunoreactivity in actively demyelinating lesions and upregulation of AQP4 in chronic inactive lesions in NMO/NMOSD cases

Five NMO cases (NMO-2, 3, 4, 7 and 10) and an NMOSD case showed preferential loss of AQP4 in at least one of the actively demyelinating lesions beyond the demyelinated areas (Pattern A) (Figure 1, Table 4). NMO-10, with known anti-AQP4 antibody seropositivity, showed extensive AQP4 loss, not only in the lesion center where numerous myelin-laden foamy macrophages had infiltrated (Figure 1D), but also in the surrounding, GFAP-immunopositive myelinated areas (Figure 1A–C). In actively demyelinating lesions, GFAP immunostaining revealed highly degenerated astrocytic vascular foot processes (Figure 1E), and AQP4 expression was totally lost in these GFAP-immunopositive structures (Figure 1F).

In addition to the actively demyelinating lesions and necrotic lesions (Figure 1G, dagger, Figure 1K), still-myelinated areas at the lesion periphery occasionally showed a remarkable decrease in both GFAP and AQP4 expression in Pattern A, which was considered to represent early lesions (Figure 1G–O, asterisk in G). In such lesions, GFAP immunostaining revealed remaining highly degenerated astrocytes and their vascular foot processes (Figure 1N). Despite the existence of remnant astrocytes, AQP4 immunoreactivity was hardly detectable in such lesions (Figure 1O).

In contrast to the loss of both GFAP and AQP4 expression in acute lesions in this group, all the chronic inactive lesions in the NMO/NMOSD cases, including those in the anti-AQP4 antibody-seropositive case (NMO-10; Figure 2A–D), showed upregulation of AQP4 in areas with various degrees of reparative gliosis (either Pattern C or D) (Figure 2, Table 4).

Preserved AQP4 expression in actively demyelinating lesions in NMO cases

While the above-mentioned cases showed typical AQP4 and GFAP loss in active demyelinating lesions as reported previously (38, 45), five cases (NMO-1, 5, 6, 8 and 9) showed no preferential loss of AQP4 (Pattern D) in any lesions, including actively demyelinating lesions except for necrotic or cavitary lesions where no astrocytes were present (Pattern N) (Figure 3D–F, Table 4).

Heterogeneous AQP4 expression in actively demyelinating lesions

Among the NMO cases with preferential loss of AQP4 (Pattern A or B) in active lesions, we found a subset of cases showing lesion-to-lesion heterogeneity in AQP4 expression pattern, even among the active lesions (Figure 3G–L; compare with Figure 1G–O, Table 4). These included three NMO cases (NMO-4, 7 and 10) and one NMOSD case. Pattern D was observed in an active lesion in one case (NMO-4), and Pattern C was observed in chronic active lesions in five cases (NMO-2, 3, 4, 7 and 10) (Table 4). The NMO-4 case had repeated attacks of transverse myelitis and acutely developed a single episode of bilateral optic neuritis 1 month prior to death. As described earlier, the corpus callosum contained partially necrotized actively demyelinating lesions, with diminished AQP4 immunoreactivity extending over the loss of myelin staining and areas with reactive astrocytes, representing Patterns A and N (Figure 1G–O). Approximately half of the actively demyelinating lesions in this case were classified as Pattern A (Table 4). By contrast, the optic chiasm had actively demyelinating lesions densely infiltrated with macrophages containing myelin debris (Figure 3G–I), where both GFAP and AQP4 was expressed diffusely in the demyelinated lesions and the surrounding normal-looking areas (Figure 3J, K). At higher magnification, the demyelinating lesions were diffusely stained for AQP4 (Figure 3L) in many hypertrophic astrocytes and their processes, being classified as Pattern D.

Immunohistochemical findings in MS

Three MS cases (MS-1, 2 and 5) showed preservation of AQP4 in actively demyelinating lesions, whereas the other two (MS-3 and 4) showed preferential AQP4 loss in active lesions of both acute and chronic stages (Pattern A or B) (Table 5). All the MS cases showed AQP4 immunoreactivity in gliotic areas of chronic inactive lesions, if present (Pattern C or D) (Table 5).

Preferential decrease of AQP4 staining in actively demyelinating lesions

The MS-3 case had cerebral signs at disease onset and brainstem signs at relapse, but neither optic neuritis nor myelitis was noted.

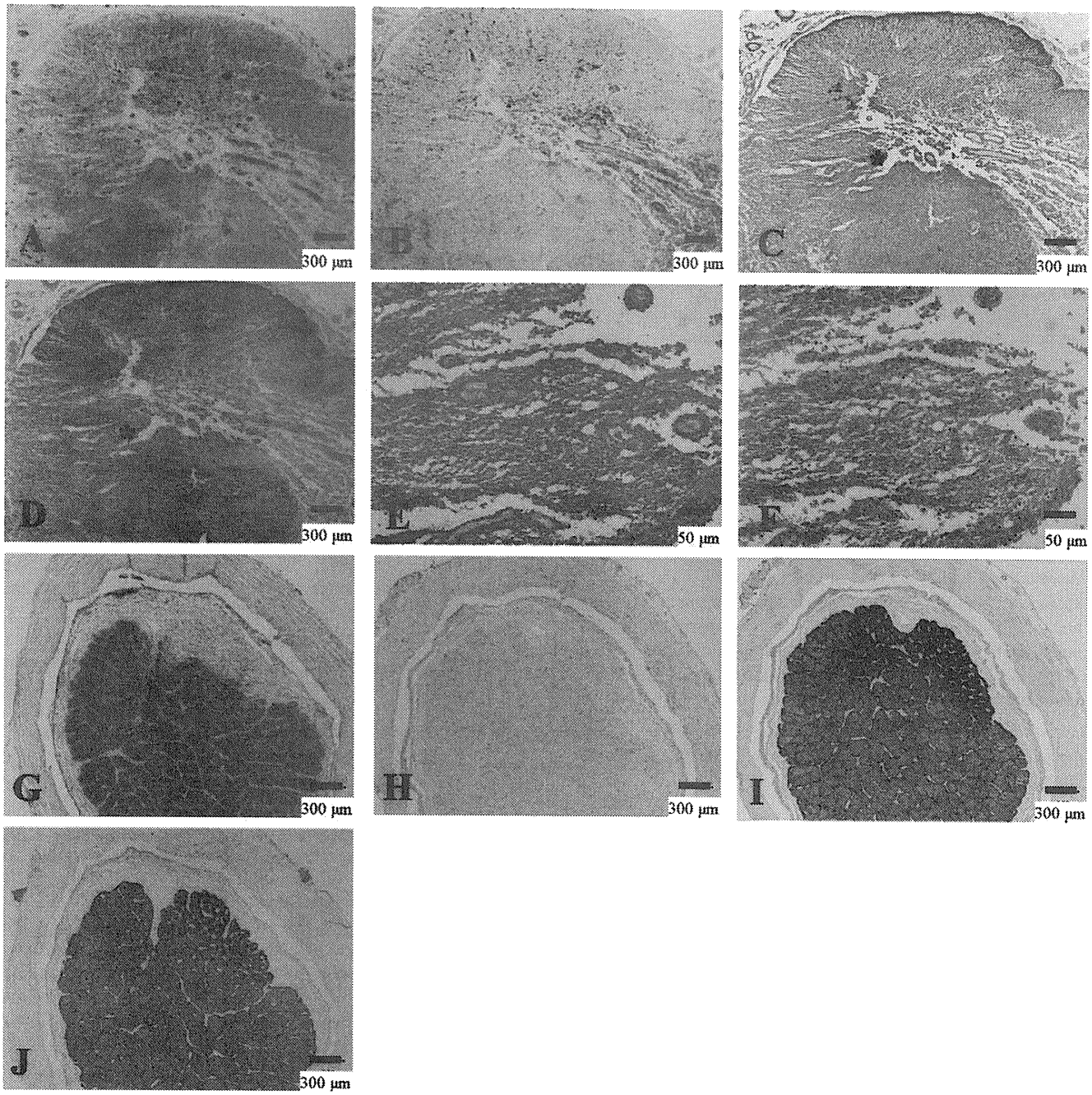

Figure 2. Upregulation of AQP4 in chronic NMO lesions. (**A–F**) Serial sections of chronic active demyelinating lesions in the spinal cord of NMO-10 representing Pattern C and N. **A.** The spinal cord has irregularly-shaped demyelinating lesions with necrosis and cavity formation. Reactive proliferation of capillary vessels is noted. **B.** CD68-positive macrophages are still abundant in the perivascular regions. **C.** The lesion is immunopositive for GFAP except for in the cavity center. **D.** Upregulation of AQP4 in extensively demyelinated lesions. **E.** High magnification in the lesion indicated by the asterisk in C shows increased GFAP immunoreactivity. **F.** The same area as E demonstrates AQP4 staining in areas of astrogliosis. (**G–J**) Serial sections of chronic inactive demyelinating lesions in the optic nerve from NMOSD, representing Pattern D. **G.** Sharply demarcated demyelinating plaque in the optic nerve. **H.** Macrophage infiltration is absent. **I.** GFAP-positive chronic astrogliosis covers the demyelinating plaque. **J.** AQP4 expression is upregulated in the areas of chronic astrogliosis. **A, G**, KB staining; **B, H**, CD68 immunohistochemistry (IHC); **C, E, I**, GFAP IHC; **D, F, J**, AQP4 IHC. Scale bar = 300 μm (**A–D, G–J**); 50 μm (**E, F**). AQP4 = aquaporin-4; GFAP = glial fibrillary acidic protein; KB = Klüver-Barrera staining; NMO = neuromyelitis optica; NMOSD = NMO spectrum disorder.

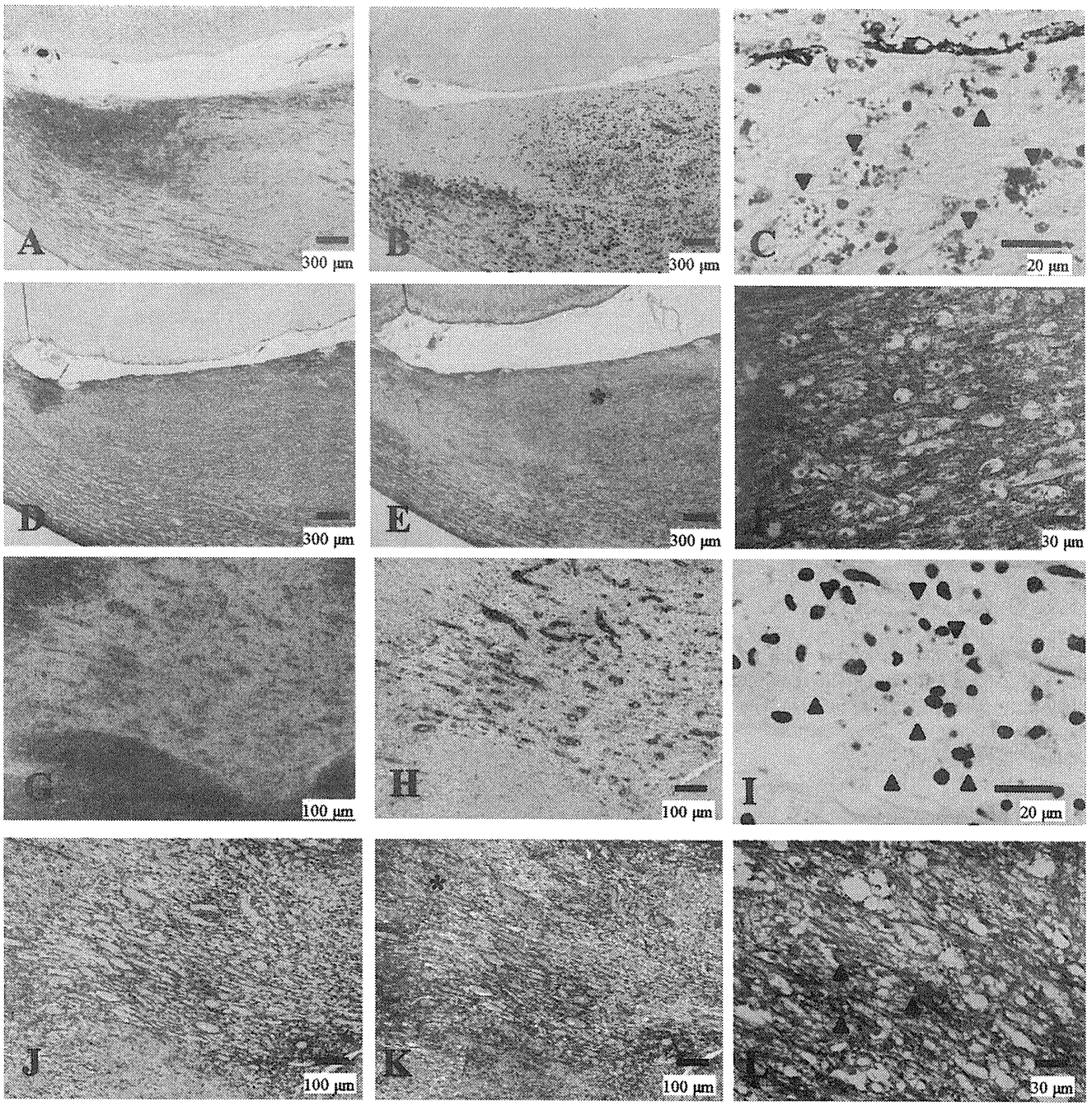

Figure 3. Preserved AQP4 immunoreactivity in actively demyelinating NMO lesions. (**A–F**) Serial sections of an actively demyelinating lesion from NMO-6 representing Pattern D. **A.** Demyelinating plaque in the corpus callosum. **B.** The lesion is infiltrated by numerous foamy macrophages stained with CD68. **C.** Macrophages containing myelin debris (arrowheads). **D.** The lesion shows strong GFAP immunoreactivity. **E.** The same area as in **D**, with AQP4 expression as strong and diffuse as that of GFAP. **F.** High magnification of the area indicated by the asterisk in **E.** AQP4 expression is preserved despite dense macrophage infiltration. (**G–L**) Serial sections of an optic nerve lesion from NMO-4 representing Pattern D. **G.** Sharply demarcated demyelinating plaques are seen. **H.** The optic chiasm is densely infiltrated with foamy macrophages. **I.** Numerous macrophages contain myelin debris. **J.** Numerous GFAP-positive reactive astrocytes in the lesion center and the surrounding areas. **K.** AQP4 immunoreactivity is enhanced at the lesion center. **L.** High magnification of the area indicated by the asterisk in **K** demonstrates AQP4 staining along the entire processes and outlining the cytoplasm of hypertrophic reactive astrocytes (arrowheads). **A, C, G, I**, KB staining; **B, H**, CD68 immunohistochemistry (IHC); **D, J**, GFAP IHC; **E, F, K, L**, AQP4 IHC. Scale bar = 300 μm (**A, B, D, E**); 100 μm (**G, H, J, K**);30 μm (**F, L**); 20 μm (**C, I**). AQP4 = aquaporin-4; GFAP = glial fibrillary acidic protein; KB = Klüver-Barrera staining; NMO = neuromyelitis optica.

Table 5. Summary of aquaporin-4 immunoreactivity patterns in demyelinating lesions in cases with multiple sclerosis. Abbreviations: AQP4 = aquaporin-4; MS = multiple sclerosis.

Autopsy	Stage	Cerebrum	Brainstem	Cerebellum	Spinal cord	Optic nerve
Preferential AQP4 loss or decrease						
MS-3	Active	A&N (1), B (3), B&N (1), N (1)	A&N (2), N (2)			
	Chronic active	B (2)				
	Chronic inactive	C (1)				
MS-4	Active		A (1), B (3)			
	Chronic active		B (1)		A &N (3), A (1)	C (1)
Preserved AQP4 expression						
MS-1	Active		N (3)			
	Chronic active	D&N (1)				
	Chronic inactive				D (1), D&N (2)	
MS-2	Active		D (1), D&N (1)			D (1)
	Chronic active		D (2)			D (1)
MS-5	Active	D (2)	D (1)	D (1)		
	Chronic active	D (1)	D (1)			
	Chronic inactive	D (4), D&N (3)		D (1)		D (1)

Blank cell = no lesions.

Notably, AQP4 loss was observed in both the centers of actively demyelinating plaques with dense perivascular lymphocytic cuffing in the cerebral peduncle, and in the periphery of the lesions where KB staining indicated preserved myelin with diffuse macrophage infiltration. This lesion was thus classified as Pattern A (see asterisks in Figure 4A–D). At higher magnification, GFAP immunostaining revealed degeneration of astrocytes and disruption of the perivascular glia limitants (Figure 4E). AQP4 expression was almost totally lost even in the scattered GFAP-positive structures (Figure 4F).

Loss of AQP4 expression in BCS-like concentric spinal cord lesions in an MS case

MS-4 had concentric lesions showing alternating rings with and without myelin in the chronic active stage, accompanied by perivascular macrophage infiltration in the spinal cord (Figure 4G, H). AQP4 loss was seen not only in the sharply demyelinated layers but also in the preserved myelin layers, and this lesion was classified as Pattern A (Figure 4I, J). High magnification demonstrated that AQP4 expression was lost on the astrocytic processes and reactive astrocytes, even though they were positive for GFAP (Figure 4K, L).

The actively demyelinating lesions in these two cases were classified as Pattern A or B (loss of AQP4).

Relationship between complement and immunoglobulin deposition and AQP4 loss

In the actively demyelinating lesions of the NMO/NMOSD cases, depositions of activated complement and immunoglobulins in the perivascular areas were observed in 28.6% of Pattern A lesions (Figures 5A–H and 7A). In chronic active lesions, such depositions were noted in 10%–15% of Patterns A, B and C. In chronic inactive lesions, one of 17 (6%) Pattern D lesions had perivascular deposits. However, MS cases did not have depositions in any demyelinated lesion (Figure 5I, J).

Four of the six cases with NMO/NMOSD that had AQP4 loss (Pattern A) showed concurrent perivascular deposition of activated complement and immunoglobulins in at least one actively

Figure 4. Preferential loss of AQP4 immunoreactivity in MS. **(A–F)** Serial sections of actively demyelinating lesions in the midbrain of MS-3 without optic-spinal lesions representing Patterns A & N. **A.** A demyelinating plaque in the acute stage in the cerebral peduncle, with dense perivascular lymphocytic cuffing. Myelin is still preserved at the periphery of the lesion (asterisk) despite CD68-positive foamy macrophage infiltration (**B**). **C.** GFAP immunoreactivity is decreased in the lesion center while numerous reactive astrocytes are present at the lesion edge and surrounding areas (asterisk). **D.** AQP4 immunoreactivity is extensively lost in not only the demyelinating center but also in the surrounding areas, where GFAP immunoreactivity is preserved (asterisk). **E.** High magnification of the area indicated by an arrowhead in C and D. Vascular foot processes are destroyed but there are remaining GFAP-positive astrocytes. **F.** The same microscopic field as in **E.** Astrocytes are devoid of AQP4 immunoreactivity. **(G–L)** Serial sections of chronic active Baló-like concentric lesions in the spinal cord from MS-4 representing Pattern A. **G.** The spinal cord shows concentric bands of alternating demyelination and preserved myelin. **H.** CD68-positive macrophages are still abundant in the lesions. **I.** GFAP immunostaining indicates strong gliosis at the lesion edge and surrounding areas. **J.** AQP4 immunoreactivity is completely lost in the lesion center and the surrounding area with preserved myelin staining (note the AQP4-immunopositive area only at the periphery of the spinal cord). **K.** High magnification of the blood vessels indicated by the arrowhead in **I** and **J** shows numerous GFAP-positive reactive astrocytes and remnant astrocytic vascular foot processes. **L.** In the same area as **K**, AQP4 immunoreactivity is completely lost in the GFAP-positive structures. **A, G**, KB; **B, H**, CD68 immunohistochemistry (IHC); **C, E, I, K**, GFAP IHC; **D, F, J, L**, AQP4 IHC. Scale bar = 500 μm **(G–J)**; 300 μm **(A–D)**; 50 μm **(E, F)**; 30 μm **(K, L)**. AQP4 = aquaporin-4; GFAP = glial fibrillary acidic protein; KB = Klüver-Barrera staining; MS = multiple sclerosis.

demyelinating lesion. This represented 36% (4/11) of all NMO/NMOSD cases (Figure 7C). All of these cases demonstrated heterogeneity in the relationship between AQP4 loss and perivascular deposition of activated complement and immunoglobulins. Moreover, we also observed different patterns of AQP4 loss and perivascular deposition of activated complement and immunoglobulins even within a single lesion. For example, in NMO-10 with anti-AQP4 antibody, in the active cerebral lesions where AQP4 was totally lost, there was no deposition of either immunoglobulin or complement (Figure 5E–H). On the other hand, in the peripheral area of a chronic active demyelinating lesion (Pattern C) in the cerebral white matter, there were blood vessels surrounded by myelin showing variable degrees of diminished staining (Figure 6A). There was no macrophage infiltration or decreased AQP4 immunoreactivity in this area (Figure 6B, C), despite deposition of activated complement and immunoglobulins around some blood vessels (Figure 6D–G). Another chronic inactive lesion in the cerebral white matter, where AQP4 immunoreactivity was markedly increased (Figure 6H–J), showed perivascular deposits of activated complement and

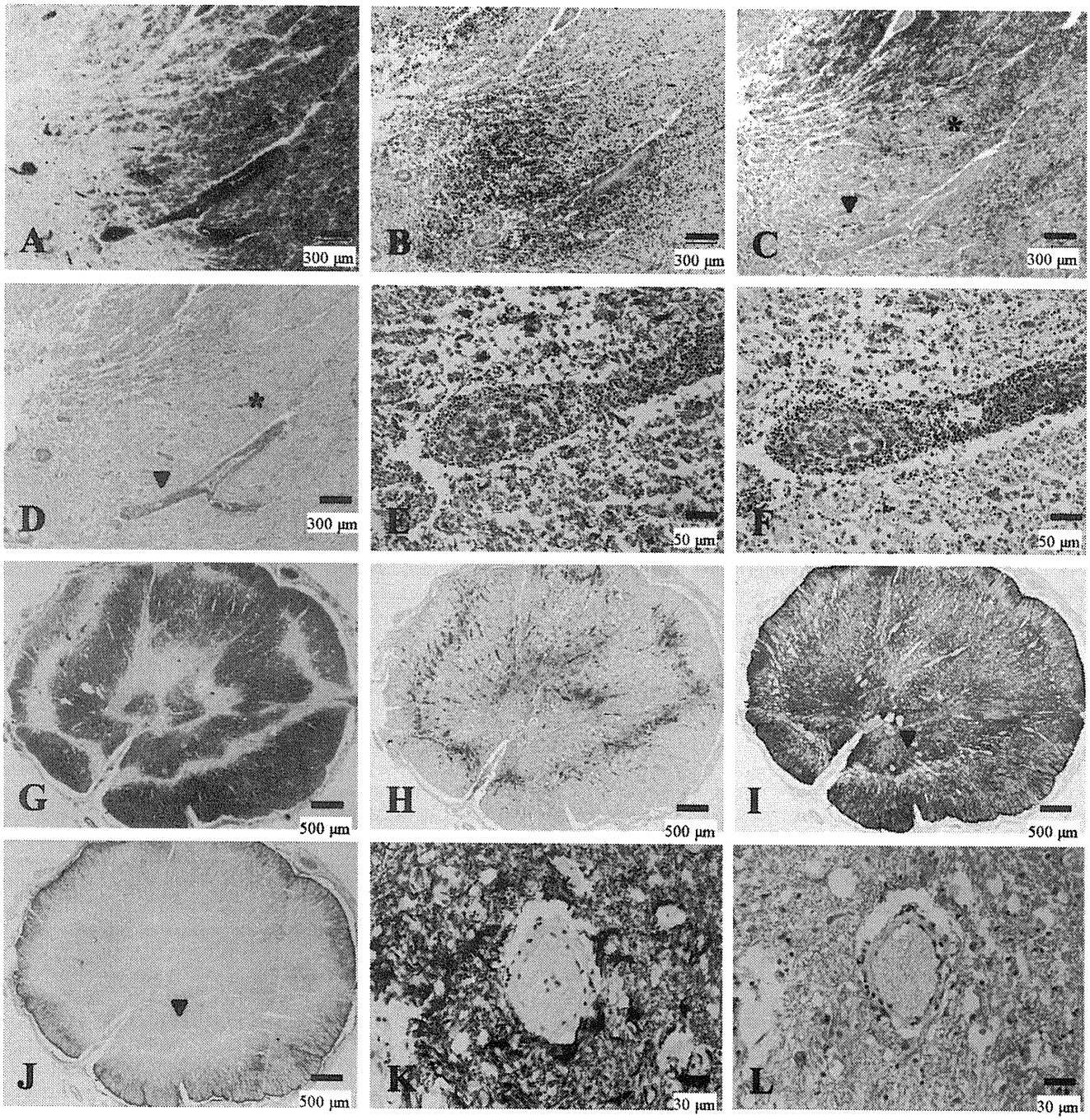

Table 6-1. Frequency of each aquaporin-4 immunoreactivity pattern in demyelinating lesions from cases with neuromyelitis optica (NMO) or NMO spectrum disorders Abbreviations: NMO = neuromyelitis optica; NMOSD = neuromyelitis optica spectrum disorder

Lesion pattern	NMO and NMOSD (n = 149)		
	Active (n = 42)	Chronic active (n = 72)	Chronic inactive (n = 35)
Pattern A	17	13	0
Pattern B	10	12	0
Pattern C	0	11	9
Pattern D	9	36	23
Pattern N	6	0	3

Table 6-2. Frequency of each aquaporin-4 immunoreactivity pattern in demyelinating lesions from cases with multiple sclerosis Abbreviations: MS = multiple sclerosis.

Lesion pattern	MS (n = 51)		
	Active (n = 24)	Chronic active (n = 14)	Chronic inactive (n = 13)
Pattern A	4	4	0
Pattern B	7	3	0
Pattern C	0	1	1
Pattern D	7	6	12
Pattern N	6	0	0

See Table 3 for the definition of the patterns. Any pattern with necrosis- (Patterns X and N) was included into Pattern X.

immunoglobulins (Figure 6K, L). However, chronic active lesions in the spinal cord demonstrated loss of AQP4 immunoreactivity with perivascular staining for complement and immunoglobulins (Figure 6M–O).

Areas with complement and immunoglobulin deposition, but without either demyelination or AQP4 loss (as shown in Figure 6B–G), were noted in five cases (three of the four NMO/NMOSD cases that showed concurrent perivascular complement and immunoglobulin deposition and AQP4 loss in some lesions, and one NMO/NMOSD case and one MS case that showed perivascular complement and immunoglobulin deposition, but neither AQP4 loss nor demyelination).

Relationship between perivascular lymphocytic cuffing and AQP4 loss

The frequency of each AQP4 expression pattern is summarized in Table 6. In actively demyelinating lesions, 23 of 38 (60.5%) Pattern A or B lesions (51.9% in NMO/NMOSD and 81.8% in MS) and eight of 16 (50.0%) Pattern D lesions (55.6% in NMO/NMOSD, and 42.9% in MS) showed perivascular lymphocytic cuffing. In total, perivascular cuffing was observed in 60% of the actively demyelinating lesions, regardless of clinical phenotype or AQP4 status (Figures 5K–M and 7B). In chronic active lesions, seven of 32 (21.9%) Pattern A or B lesions (16.0% in NMO/NMOSD and 42.9% in MS) and six of 42 (14.3%) Pattern D lesions (13.9% in NMO/NMOSD and 16.7% in MS) demonstrated perivascular lymphocytic cuffing. Generally, lymphocytic cuffing was milder in NMO/NMOSD than in MS. In addition, all lesions had predominant T-cell infiltration (30 in actively demyelinating lesions and 12 in chronic active lesions) (see Figure 5K–M).

DISCUSSION

We performed a systematic immunohistopathological study on autopsied cases of NMO and MS. Half of NMO patients showed preferential loss of AQP4 beyond the area of demyelination, whereas others did not, even in actively demyelinating lesions. Some MS patients, including one with only brain lesions and the other with BCS-like concentric spinal cord lesions, demonstrated extensive AQP4 loss in actively demyelinating and chronic active lesions, whereas other MS patients showed preservation of AQP4. Even NMO and MS patients with preferential AQP4 loss showed AQP4 patterns that varied from lesion to lesion, with no AQP4 loss in some of the actively demyelinating lesions, as well as in chronic active and inactive lesions. Vasculocentric deposition of complement and immunoglobulins was specifically noted in a third of NMO/NMOSD cases, but did not tightly correlate with perivascular AQP4 loss. Overall, our study indicates that antibody and

Figure 5. Distinctive patterns of perivascular immunoglobulin/complement deposition and lymphocytic cuffing between NMO and MS. (**A–D**) Active lesions in NMO with immunoglobulin/complement deposition. (**A, B**) Serial sections of a periplaque, still-myelinated area of NMO-4. These figures show the same area as that indicated by the arrowhead in Figure 1, G and I. IgM (**A**) and C3d (**B**) deposition are observed in astrocytic vascular foot processes as well as in degenerated astrocytes (arrowheads). (**C, D**) Serial sections from a more advanced active lesion in the spinal cord from NMO-7. IgG (**C**) and IgM (**D**) deposition are observed in astrocytic vascular foot processes as well as degenerated astrocytes (arrowheads). (**E–H**) Serial sections of an active lesion from NMO-10 without immunoglobulin/complement deposition. These figures show the periplaque, still-myelinated areas of the lesion shown in Figure 1A–F. Although GFAP immunoreactivity is preserved (**E**), AQP4 expression is totally lost (**F**). Neither C9neo (**G**) nor IgG (**H**) staining shows specific perivascular deposition. (**I, J**) Lack of immunoglobulin/complement deposition in MS. Serial sections of a chronic active lesion from MS-4. These figures show the same area as in Figure 4K and L. Neither IgG (**I**) nor C3d (**J**) staining shows typical perivascular deposition. (**K–M**) Lymphocyte cuffing in MS and NMO. (**K, L**) Serial sections from an active lesion from MS-3. These figures show the same lesion as in Figure 4E and F. **K.** CD45RO staining demonstrates perivascular cuffing predominantly consisting of T cells. **L.** Few CD20-positive B cells in the perivascular area. **M.** An active lesion in the spinal cord from NMO-7. This figure shows the same lesion as in **C** and **D**. Although CD45RO-positive T-cells predominate, the degree of perivascular lymphocyitic accumulation is much milder in NMO than in MS. **A, D**, IgM immunohistochemistry (IHC); **B, J**, C3d IHC; **C, H, I**, IgG IHC; **G**, C9neo IHC; **E**, GFAP IHC; **F**, AQP4 IHC; **K, M**, CD45RO IHC, **L**, CD20 IHC. Scale bar = 100 μm (**K, L**); 50 μm (**A–J, M**). AQP4 = aquaporin-4; GFAP = glial fibrillary acidic protein; KB = Klüver-Barrera staining; MS = multiple sclerosis; NMO = neuromyelitis optica.

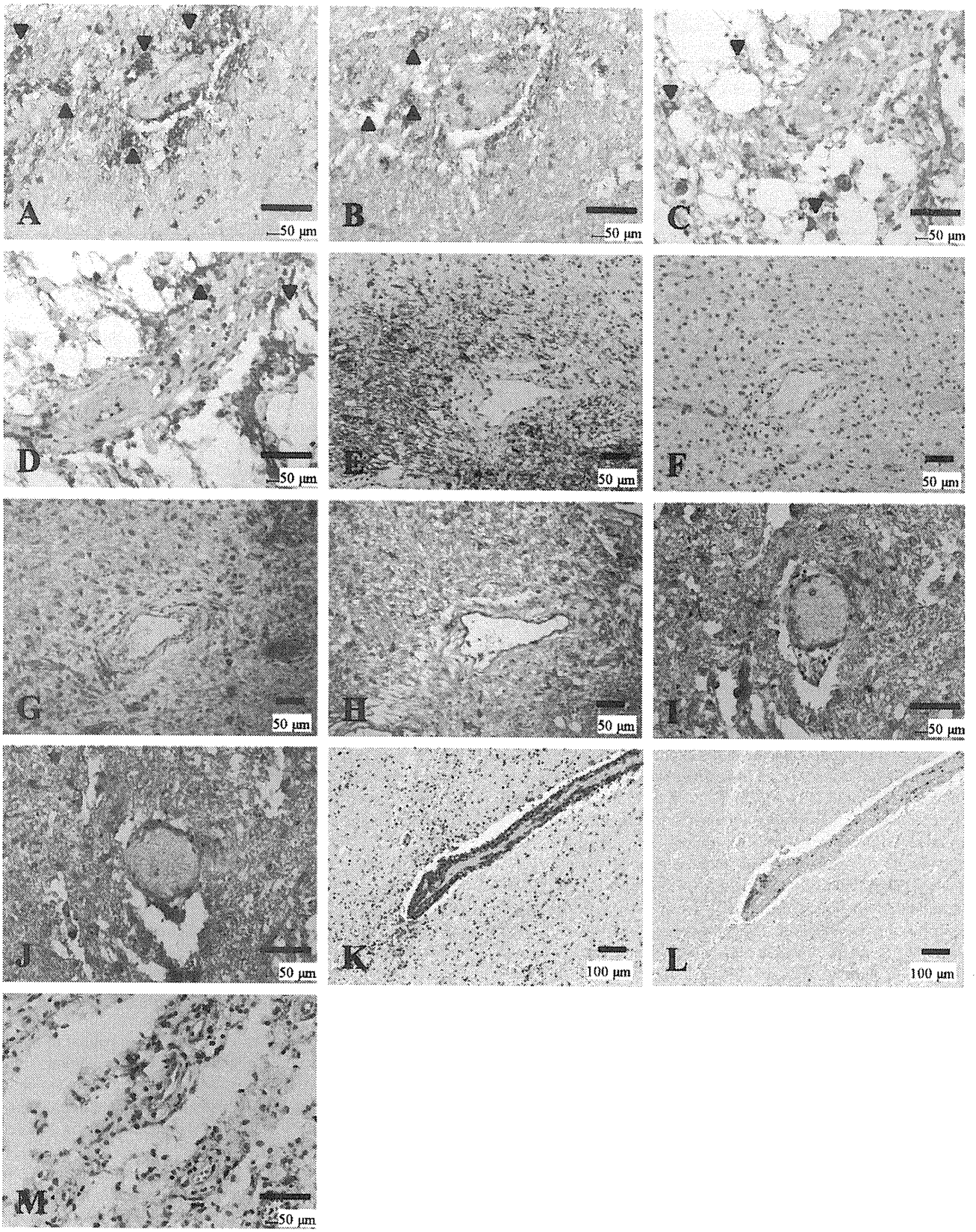

Figure 6. Heterogeneity between perivascular deposition of activated complement and immunoglobulins and AQP4 expression. (**A–G**) Serial sections of the peripheral area of chronic active lesions in the cerebral white matter of NMO-10. **A.** Demyelinating lesions confined to the vicinity of blood vessels. **B.** No inflammatory cell infiltration. **C.** AQP4 immunoreactivity on astrocyte processes. Immunoreactivities to activated complement (C3d (**D**) and C9neo (**E**)) and immunoglobulins (IgM (**F**) and IgG (**G**)) in the perivascular areas. Note that one blood vessel does not show deposition of activated complement or immunoglobulins (arrow in **D–G**). (**H–L**) Serial sections in the cerebral white matter of the same case. **H.** A chronic inactive demyelinating lesion. **I.** Few CD68-positive macrophages in the lesion. **J.** AQP4 labeling of the astrogliosis covering the lesions. C3d (**K**) and IgG (**L**) immunoreactivities are most intense in the perivascular area. (**M–O**) Serial sections of a chronic active demyelinating lesion in the spinal cord of the same case. **M.** Loss of AQP4 immunoreactivity is confined to the perivascular areas associated with C3d (**N**) and IgM (**O**) deposition. **A, H**, KB; **B, I**, CD68 immunohistochemistry (IHC); **C, J, M**, AQP4 IHC; **D, K, N**, C3d IHC; **E**, C9neo IHC; **F, O**, IgM IHC; **G, L**, IgG IHC. Scale bar = 100 μm (**A–G**); 50 μm (**H–O**); 15 μm (**C**). AQP4 = aquaporin-4; GFAP = glial fibrillary acidic protein; KB = Klüver-Barrera staining; NMO = neuromyelitis optica.

complement-related mechanisms are important in AQP4 astrocytopathy in a fraction of NMO cases, as seen in one case with anti-AQP4 antibody, but AQP4 loss can also occur in some actively demyelinating MS lesions, and can occasionally be very extensive, as seen in the Baló-like concentric spinal cord lesions of MS-4. Furthermore, the lesion-to-lesion heterogeneity in the AQP4 expression pattern observed in NMO cases implies a heterogeneous relationship between anti-AQP4 antibody and loss of AQP4 expression.

Our study has some limitations inherent to studies using archival autopsied materials. First, because the autopsied cases died with the disease, there was a potential bias toward severe cases. Our histological evaluation focusing on early active lesions and separately analyzing necrotic lesions can minimize this selection bias. Second, the anti-AQP4 antibody status was only known in one case, because the other autopsies were performed before the discovery of NMO-IgG. These limitations are common to the other pathological studies on AQP4 expression in NMO by Misu *et al* (38) and Roemer *et al* (45). We were able to evaluate AQP4 expression in the one NMO case with confirmed anti-AQP4 antibodies, which enabled a detailed evaluation of the relationship between the presence of anti-AQP4 antibody and AQP4 expression in the CNS.

The results of our study are somewhat discordant with those of previous studies (38, 45), which might, in part, be attributable to the differences in methodology and materials. Regarding the staining method, in our previous (33) and present studies, we found AQP4 expression patterns similar to those reported in normal and diseased control brain tissues (1, 27, 38, 45) despite using a different anti-AQP4 antibody. The evaluation of necrotic lesions also requires some consideration. In necrotic lesions totally replaced by macrophages where no viable astrocytes existed, we could not differentiate whether the loss of AQP4 was caused by down-modulation of AQP4 in astrocytes or the loss of astrocytes *per se*. Furthermore, in such destructive lesions, it would be difficult to determine the causal relationship between AQP4 loss and the astrocyte damage. Therefore, we decided to put more stress on evaluating earlier lesions where the background tissues were still relatively preserved. Although the clinical features of MS are somewhat different between northern (Misu's cases) and southern Japanese (our cases) (15, 41), these differences in methodology should not seriously distort our results.

Half of our NMO cases showed a preferential loss of AQP4 in actively demyelinating and chronic active lesions, whereas the rest did not, despite severe tissue destruction. This is in line with the fact that anti-AQP4 antibody is not detected in 30%–70% of NMO cases (22). Vasculocentric complement and immunoglobulin deposition was noted only in NMO/NMOSD cases but not in MS cases. These findings support the notion that AQP4 loss in NMO cases results from immune responses to AQP4 (38, 45). Accordingly, it is possible that pathologically, there are two types of NMO, namely AQP4 autoimmunity-related and AQP4 autoimmunity-unrelated, and the latter may correspond clinically to seronegative NMO (31, 35).

The vasculocentric deposition of complement and immunoglobulins was only detected in NMO patients with AQP4 loss, including one with anti-AQP4 antibody. This supports the hypothesis that anti-AQP4 antibody destroys perivascular astrocyte foot processes via complement-dependent mechanisms. However, more than half of the AQP4-down-modulated NMO lesions showed no vasculocentric deposition of complement and immunoglobulins. This might be caused by very transient complement and immunoglobulin deposition. We staged NMO lesions with myelin-laden macrophages as active according to the lesion staging in MS; however, it is possible that complement/immunoglobulin deposition rapidly disappears even in the presence of myelin-laden macrophages once it triggers the astrocytic damage. Alternatively, the findings might be interpreted, such that the anti-AQP4 antibody and complement-mediated mechanism is unique to NMO, but does not always accompany every lesion. Further studies are necessary to clarify the time course of complement/immunoglobulin deposition during the formation of NMO lesions in an experimental model.

Our pathological study also argues against autoimmune AQP4 destruction as the sole NMO mechanism. First, the severity of tissue destruction was unrelated to tissue AQP4 loss or preservation. Second, AQP4 expression was heterogeneous even in the same individual. Although chronic inactive lesions may restore AQP4 expression with astrogliosis, one NMO case showed preservation of AQP4 in actively demyelinating optic chiasmal lesions, despite reduced AQP4 expression in other CNS lesions. Third, the perivascular deposition of complement and immunoglobulins did not closely correlate with perivascular AQP4 loss.

Anti-AQP4 antibody titer could change from patient to patient and between different disease stages in the same patient, which might have affected AQP4 expression levels in the pathological lesions. However, in this case, the existence of actively demyelinating lesions without AQP4 loss in NMO patients showing preferential AQP4 loss in other active lesions suggests that anti-AQP4 antibody does not always play a primary role in initiating inflammatory lesions. Other factor(s) may be responsible for triggering the pathological features, which are then modulated by anti-AQP4 antibodies. To clarify the real consequences of this autoantibody, a prospective neuropathological study based on anti-AQP4 antibody status is required.

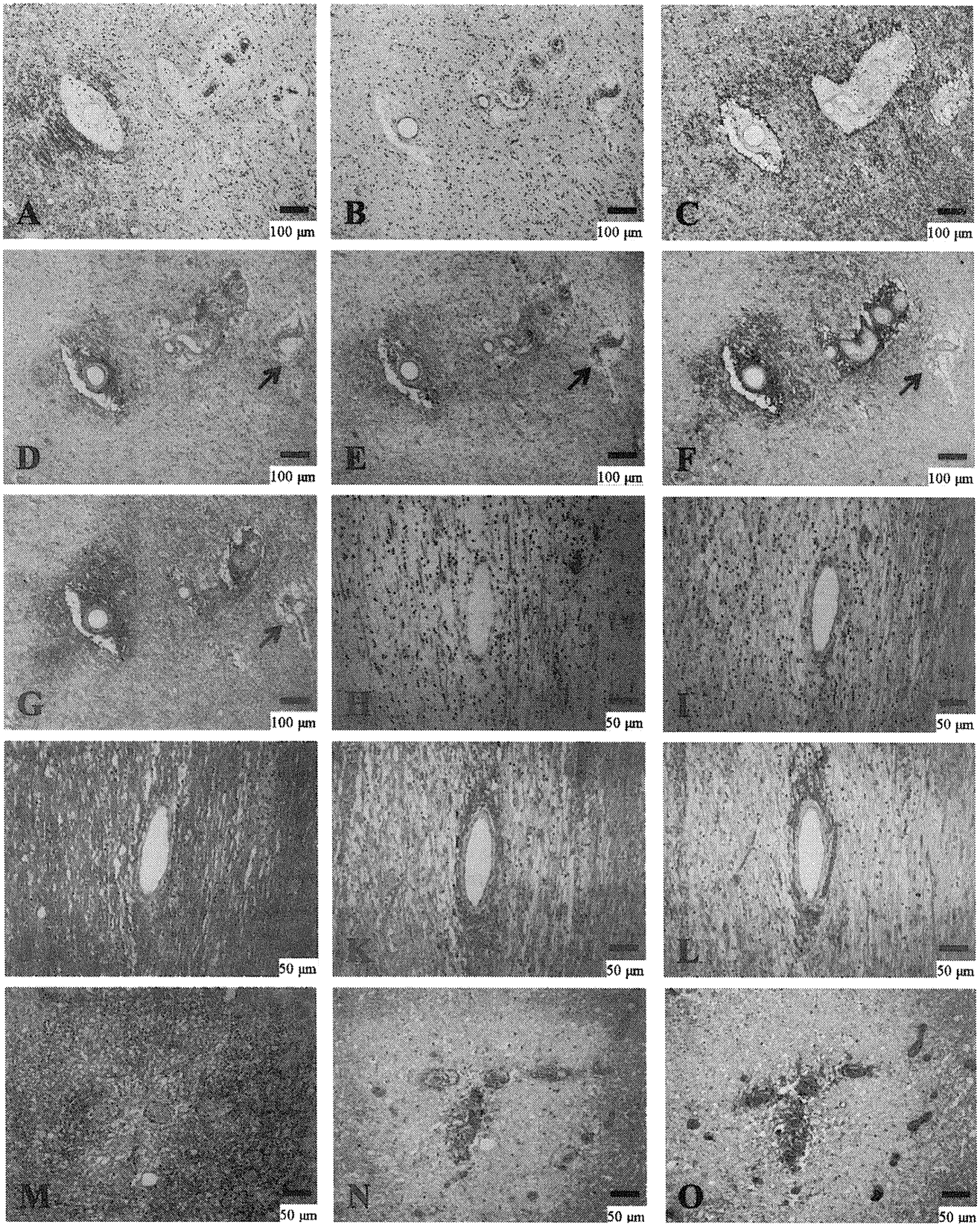

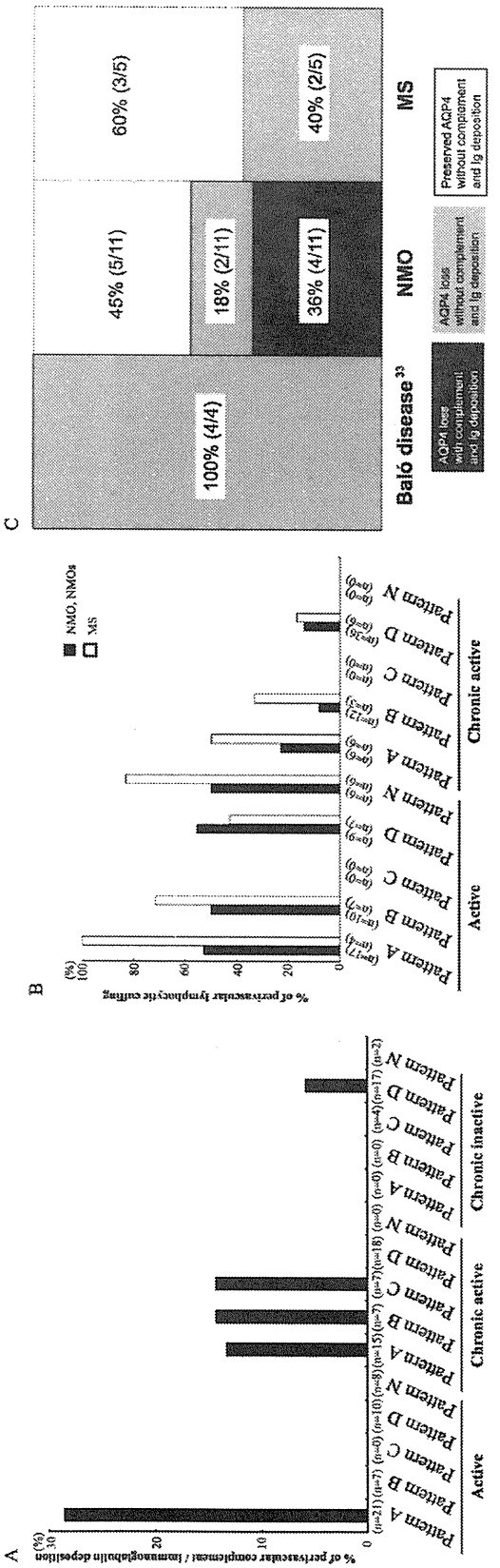

Figure 7. A. Positive rates of perivascular complement and immunoglobulin deposition in NMO/NMOSD cases according to AQP4 patterns and lesion stage. Because no MS case showed such depositions, only NMO/NMOSD lesions are included here. n = the number of demyelinating lesions. **B.** Positive rates of perivascular lymphocytic cuffing in the actively demyelinating and chronic active lesions according to AQP4 patterns and clinical phenotypes. n = the number of demyelinating lesions; see Table 3 for the definitions of the patterns. Any pattern with necrosis (Patterns X & N) was included in Pattern X. **C.** The relationship between AQP4 expression patterns and immunoglobulin/complement deposition in each disease type. The data on Baló's disease is cited from our previous report (33). AQP4 = aquaporin-4; MS = multiple sclerosis; NMO = neuromyelitis optica; NMOSD = NMO spectrum disorder.

Regarding MS, somewhat inconsistent results have been reported. Misu *et al* (38) reported no loss of AQP4 in MS plaques, whereas Roemer *et al* (45) found stage-dependent loss of AQP4, with inactive MS lesions showing complete AQP4 loss. On the other hand, Sharma *et al* (48) observed patchy AQP4 loss only in a subset of active lesions following pattern III MS lesions. These authors found loss of perivascular astrocytic foot processes where AQP4 was lost, while numerous reactive astrocytes had intense AQP4 immunoreactivity in the lesions. In our study, AQP4 expression was decreased or totally lost in acute and chronic active demyelinating lesions in a fraction of MS cases, including one that lacked optic nerve and spinal cord lesions. At the cellular level, disruption of astrocytic vascular foot processes was evident in such lesions, and AQP4 expression was lost in both cell bodies and vascular foot processes of astrocytes as seen in acute NMO lesions. Our present and previous findings (33) raise the possibility that AQP4 loss *per se* is not confined to NMO, but rather, that it could also occur in actively demyelinating lesions of MS and BCS, suggesting a notion that astrocyte damage accompanied by AQP4 loss is not always related to anti-AQP4 antibody. Sharma *et al* (48) also reported that autoantibody-independent AQP4 loss and astrocytic dysfunction occurs in lipopolysaccharide-induced experimental demyelination, providing experimental support for such a notion. Interestingly, Baló-like concentric lesions in the spinal cord of MS-4 also showed similar extensive AQP4 loss to BCS, including in the areas of preserved myelin. We previously found no vasculocentric deposition of complement and immunoglobulin in BCS cases (33), and we and others (2) also demonstrated no such perivascular deposition in MS. Thus, extensive AQP4 loss without perivascular deposition of complement and immunoglobulin may be a common pathological feature of at least a subset of the concentric lesions in BCS and MS.

In summary, antibody-mediated AQP4 astrocytopathy occurs only in NMO, whereas antibody-independent AQP4 astrocytopathy can develop in various demyelinating conditions, including MS, BCS and a fraction of NMO cases (Figure 7C). Further studies on astrocytopathy as well as the dynamic plasticity of astrocytes in demyelinating diseases may shed light on the mechanisms underlying MS and allied disorders.

ACKNOWLEDGMENTS

This work was supported in part by grants from the Research Committees of Neuroimmunological Diseases, the Ministry of Health, Labor and Welfare, Japan, and from the Ministry of Education, Culture, Sports, Science and Technology, Japan. We thank Sachiko Nagae and Kimiko Sato, Department of Neuropathology, Kyushu University, for their excellent technical assistance, and Takekazu Ohi, Department of Neurology, Kurashiki Central Hospital, for providing materials.

REFERENCES

1. Aoki K, Uchihara T, Tsuchiya K, Nakamura A, Ikeda K, Wakayama Y (2003) Enhanced expression of aquaporin 4 in human brain with infarction. *Acta Neuropathol* **106**:121–124.
2. Barnett MH, Parratt JD, Cho ES, Prineas JW (2009) Immunoglobulins and complement in postmortem multiple sclerosis tissue. *Ann Neurol* **65**:32–46.
3. Bennett JL, Lam C, Kalluri SR, Saikali P, Bautista K, Dupree C *et al* (2009) Intrathecal pathogenic anti-aquaporin-4 antibodies in early neuromyelitis optica. *Ann Neurol* **66**:617–629.
4. Bot JC, Barkhof F, Polman CH, Lycklama a Nijeholt GJ, de Groot V, Bergers E *et al* (2004) Spinal cord abnormalities in recently diagnosed MS patients: added value of spinal MRI examination. *Neurology* **62**:226–233.
5. Bradl M, Misu T, Takahashi T, Watanabe M, Mader S, Reindl M *et al* (2009) Neuromyelitis optica: pathogenicity of patient immunoglobulin *in vivo*. *Ann Neurol* **66**:630–643.
6. Cabrera-Gomez JA, Bonnan M, Gonzalez-Quevedo A, Saiz-Hinarejos A, Marignier R, Olindo S *et al* (2009) Neuromyelitis optica positive antibodies confer a worse course in relapsing-neuromyelitis optica in Cuba and French West Indies. *Mult Scler* **15**:828–833.
7. Chen CJ, Chu NS, Lu CS, Sung CY (1999) Serial magnetic resonance imaging in patients with Balo's concentric sclerosis: natural history of lesion development. *Ann Neurol* **46**:651–656.
8. Chong HT, Ramli N, Lee KH, Kim BJ, Ursekar M, Dayananda K *et al* (2006) Magnetic resonance imaging of Asians with multiple sclerosis was similar to that of the West. *Can J Neurol Sci* **33**:95–100.
9. Collongues N, Marignier R, Zephir H, Papeix C, Blanc F, Ritleng C *et al* (2010) Neuromyelitis optica in France: a multicenter study of 125 patients. *Neurology* **74**:736–742.
10. Fazio R, Malosio ML, Lampasona V, De Feo D, Privitera D, Marnetto F *et al* (2009) Antiacquaporin 4 antibodies detection by different techniques in neuromyelitis optica patients. *Mult Scler* **15**:1153–1163.
11. Graber JJ, Kister I, Geyer H, Khaund M, Herbert J (2009) Neuromyelitis optica and concentric rings of Balo in the brainstem. *Arch Neurol* **66**:274–275.
12. Hung TP, Landsborough D, Hsi MS (1976) Multiple sclerosis amongst Chinese in Taiwan. *J Neurol Sci* **27**:459–484.
13. Ikota H, Iwasaki A, Kawarai M, Nakazato Y (2010) Neuromyelitis optica with intraspinal expansion of Schwann cell remyelination. *Neuropathology* **30**:427–433.
14. Ikuta F, Koga M, Takeda S, Ohama E, Takeshita I, Ogawa H (1982) Comparison of MS pathology between 70 American and 75 Japanese autopsy cases. In: *Multiple Sclerosis East and West*, Y Kuroiwa, LT Kurland (eds), pp. 297–306. Kyushu University Press: Fukuoka.
15. Ishizu T, Kira J, Osoegawa M, Fukazawa T, Kikuchi S, Fujihara K *et al* (2009) Heterogeneity and continuum of multiple sclerosis phenotypes in Japanese according to the results of the fourth nationwide survey. *J Neurol Sci* **280**:22–28.
16. Itoyama Y, Tateishi J, Kuroiwa Y (1985) Atypical multiple sclerosis with concentric or lamellar demyelinated lesions: two Japanese patients studied post mortem. *Ann Neurol* **17**:481–487.
17. Jarius S, Franciotta D, Bergamaschi R, Wright H, Littleton E, Palace J *et al* (2007) NMO-IgG in the diagnosis of neuromyelitis optica. *Neurology* **68**:1076–1077.
18. Jung JS, Bhat RV, Preston GM, Guggino WB, Baraban JM, Agre P (1994) Molecular characterization of an aquaporin cDNA from brain: candidate osmoreceptor and regulator of water balance. *Proc Natl Acad Sci U S A* **91**:13052–13056.
19. Kinoshita M, Nakatsuji Y, Kimura T, Moriya M, Takata K, Okuno T *et al* (2009) Neuromyelitis optica: passive transfer to rats by human immunoglobulin. *Biochem Biophys Res Commun* **386**:623–627.
20. Kinoshita M, Nakatsuji Y, Moriya M, Okuno T, Kumanogoh A, Nakano M *et al* (2009) Astrocytic necrosis is induced by anti-aquaporin-4 antibody-positive serum. *Neuroreport* **20**:508–512.
21. Kinoshita M, Nakatsuji Y, Kimura T, Moriya M, Takata K, Okuno T *et al* (2010) Anti-aquaporin-4 antibody induces astrocytic cytotoxicity

in the absence of CNS antigen-specific T cells. *Biochem Biophys Res Commun* **394**:205–210.
22. Kira J (2010) Neuromyelitis optica and opticospinal multiple sclerosis: mechanisms and pathogenesis. *Pathophysiology* **18**:69–79.
23. Kishimoto R, Yabe I, Niino M, Sato K, Tsuji S, Kikuchi S, Sasaki H (2008) Balo's concentric sclerosislike lesion in the brainstem of a multiple sclerosis patient. *J Neurol* **255**:760–761.
24. Kobayashi Z, Tsuchiya K, Uchihara T, Nakamura A, Haga C, Yokota O *et al* (2009) Intractable hiccup caused by medulla oblongata lesions: a study of an autopsy patient with possible neuromyelitis optica. *J Neurol Sci* **285**:241–245.
25. Kuroiwa Y (1985) Neuromyelitis optica (Devic's disease, Devic's syndrome. In. *Handbook of Clinical Neurology Vol. 3: Demyelinating Diseases*, JC Koetsier (ed.), pp. 397–408. Elsevier Science Publishers: Amsterdam.
26. Lassmann H, Raine CS, Antel J, Prineas JW (1998) Immunopathology of multiple sclerosis: report on an international meeting held at the Institute of Neurology of the University of Vienna. *J Neuroimmunol* **86**:213–217.
27. Lee TS, Eid T, Mane S, Kim JH, Spencer DD, Ottersen OP, de Lanerolle NC (2004) Aquaporin-4 is increased in the sclerotic hippocampus in human temporal lobe epilepsy. *Acta Neuropathol* **108**:493–502.
28. Lennon VA, Wingerchuk DM, Kryzer TJ, Pittock SJ, Lucchinetti CF, Fujihara K *et al* (2004) A serum autoantibody marker of neuromyelitis optica: distinction from multiple sclerosis. *Lancet* **364**:2106–2112.
29. Lennon VA, Kryzer TJ, Pittock SJ, Verkman AS, Hinson SR (2005) IgG marker of optic-spinal multiple sclerosis binds to the aquaporin-4 water channel. *J Exp Med* **202**:473–477.
30. Lucchinetti CF, Mandler RN, McGavern D, Bruck W, Gleich G, Ransohoff RM *et al* (2002) A role for humoral mechanisms in the pathogenesis of Devic's neuromyelitis optica. *Brain* **125**:1450–1461.
31. Matsuoka T, Matsushita T, Kawano Y, Osoegawa M, Ochi H, Ishizu T *et al* (2007) Heterogeneity of aquaporin-4 autoimmunity and spinal cord lesions in multiple sclerosis in Japanese. *Brain* **130**:1206–1223.
32. Matsuoka T, Matsushita T, Osoegawa M, Ochi H, Kawano Y, Mihara F *et al* (2008) Heterogeneity and continuum of multiple sclerosis in Japanese according to magnetic resonance imaging findings. *J Neurol Sci* **266**:115–125.
33. Matsuoka T, Suzuki SO, Iwaki T, Tabira T, Ordinario AT, Kira J (2010) Aquaporin-4 astrocytopathy in Baló's disease. *Acta Neuropathol* **120**:651–660.
34. Matsushita T, Isobe N, Matsuoka T, Ishizu T, Kawano Y, Yoshiura T *et al* (2009) Extensive vasogenic edema of anti-aquaporin-4 antibody-related brain lesions. *Mult Scler* **15**:1113–1117.
35. Matsushita T, Isobe N, Matsuoka T, Shi N, Kawano Y, Wu XM *et al* (2009) Aquaporin-4 autoimmune syndrome and anti-aquaporin-4 antibody-negative opticospinal multiple sclerosis in Japanese. *Mult Scler* **15**:834–847.
36. Matsushita T, Isobe N, Piao H, Matsuoka T, Ishizu T, Doi H *et al* (2010) Reappraisal of brain MRI features in patients with multiple sclerosis and neuromyelitis optica according to anti-aquaporin-4 antibody status. *J Neurol Sci* **291**:37–43.
37. Minohara M, Matsuoka T, Li W, Osoegawa M, Ishizu T, Ohyagi Y, Kira J (2006) Upregulation of myeloperoxidase in patients with opticospinal multiple sclerosis: positive correlation with disease severity. *J Neuroimmunol* **178**:156–160.
38. Misu T, Fujihara K, Kakita A, Konno H, Nakamura M, Watanabe S *et al* (2007) Loss of aquaporin 4 in lesions of neuromyelitis optica: distinction from multiple sclerosis. *Brain* **130**:1224–1234.
39. Nakashima I, Fujihara K, Miyazawa I, Misu T, Narikawa K, Nakamura M *et al* (2006) Clinical and MRI features of Japanese patients with multiple sclerosis positive for NMO-IgG. *J Neurol Neurosurg Psychiatry* **77**:1073–1075.
40. Okinaka S, Tsubaki T, Kuroiwa Y, Toyokura Y, Imamura Y (1958) Multiple sclerosis and allied diseases in Japan; clinical characteristics. *Neurology* **8**:756–763.
41. Osoegawa M, Kira J, Fukazawa T, Fujihara K, Kikuchi S, Matsui M *et al* (2009) Temporal changes and geographical differences in multiple sclerosis phenotypes in Japanese: nationwide survey results over 30 years. *Mult Scler* **15**:159–173.
42. Paul F, Jarius S, Aktas O, Bluthner M, Bauer O, Appelhans H *et al* (2007) Antibody to aquaporin 4 in the diagnosis of neuromyelitis optica. *PLoS Med* **4**:e133.
43. Pittock SJ, Lennon VA, Krecke K, Wingerchuk DM, Lucchinetti CF, Weinshenker BG (2006) Brain abnormalities in neuromyelitis optica. *Arch Neurol* **63**:390–396.
44. Poser CM, Paty DW, Scheinberg L, McDonald WI, Davis FA, Ebers GC *et al* (1983) New diagnostic criteria for multiple sclerosis: guidelines for research protocols. *Ann Neurol* **13**:227–231.
45. Roemer SF, Parisi JE, Lennon VA, Benarroch EE, Lassmann H, Bruck W *et al* (2007) Pattern-specific loss of aquaporin-4 immunoreactivity distinguishes neuromyelitis optica from multiple sclerosis. *Brain* **130**:1194–1205.
46. Saadoun S, Waters P, Bell BA, Vincent A, Verkman AS, Papadopoulos MC (2010) Intra-cerebral injection of neuromyelitis optica immunoglobulin G and human complement produces neuromyelitis optica lesions in mice. *Brain* **133**:349–361.
47. Sabater L, Giralt A, Boronat A, Hankiewicz K, Blanco Y, Llufriu S *et al* (2009) Cytotoxic effect of neuromyelitis optica antibody (NMO-IgG) to astrocytes: an *in vitro* study. *J Neuroimmunol* **215**:31–35.
48. Sharma R, Fischer MT, Bauer J, Felts PA, Smith KJ, Misu T *et al* (2010) Inflammation induced by innate immunity in the central nervous system leads to primary astrocyte dysfunction followed by demyelination. *Acta Neuropathol* **120**:223–236.
49. Su JJ, Osoegawa M, Matsuoka T, Minohara M, Tanaka M, Ishizu T *et al* (2006) Upregulation of vascular growth factors in multiple sclerosis: correlation with MRI findings. *J Neurol Sci* **243**:21–30.
50. Tabira T, Tateishi J (1982) Neuropathological features of MS in Japan. In: *Multiple Sclerosis East and West*, Y Kuroiwa, LT Kurland (eds), pp. 273–295. Kyushu University Press: Fukuoka.
51. Viegas S, Weir A, Esiri M, Kuker W, Waters P, Leite MI *et al* (2009) Symptomatic, radiological and pathological involvement of the hypothalamus in neuromyelitis optica. *J Neurol Neurosurg Psychiatry* **80**:679–682.
52. Vincent T, Saikali P, Cayrol R, Roth AD, Bar-Or A, Prat A, Antel JP (2008) Functional consequences of neuromyelitis optica-IgG astrocyte interactions on blood-brain barrier permeability and granulocyte recruitment. *J Immunol* **181**:5730–5737.
53. Wang CD, Zhang KN, Wu XM, Gang H, Xie XF, Qu XH, Xiong YQ (2008) Balo's disease showing benign clinical course and co-existence with multiple sclerosis-like lesions in Chinese. *Mult Scler* **14**:418–424.
54. Wingerchuk DM, Hogancamp WF, O'Brien PC, Weinshenker BG (1999) The clinical course of neuromyelitis optica (Devic's syndrome). *Neurology* **53**:1107–1114.
55. Wingerchuk DM, Lennon VA, Pittock SJ, Lucchinetti CF, Weinshenker BG (2006) Revised diagnostic criteria for neuromyelitis optica. *Neurology* **66**:1485–1489.
56. Wingerchuk DM, Lennon VA, Lucchinetti CF, Pittock SJ, Weinshenker BG (2007) The spectrum of neuromyelitis optica. *Lancet Neurol* **6**:805–815.
57. Yanagawa K, Kawachi I, Toyoshima Y, Yokoseki A, Arakawa M, Hasegawa A *et al* (2009) Pathologic and immunologic profiles of a limited form of neuromyelitis optica with myelitis. *Neurology* **73**:1628–1637.

Acta Neuropathol (2010) 120:651–660
DOI 10.1007/s00401-010-0733-7

ORIGINAL PAPER

Aquaporin-4 astrocytopathy in Baló's disease

Takeshi Matsuoka · Satoshi O. Suzuki · Toru Iwaki · Takeshi Tabira · Artemio T. Ordinario · Jun-ichi Kira

Received: 11 June 2010 / Revised: 22 July 2010 / Accepted: 27 July 2010 / Published online: 3 August 2010

Abstract Baló's concentric sclerosis (BCS) is considered to be a rare variant of multiple sclerosis and characterized by alternating rings of demyelinated and preserved myelin layers. The mechanism underlying BCS remains to be elucidated. Recently, occurrence of concentric rings of Baló was described in the brainstem of a patient with neuromyelitis optica (NMO). Because selective loss of aquaporin-4 (AQP4) and vasculocentric deposition of complement and immunoglobulins are characteristic in NMO, we aimed to assess AQP4 expression in the concentric demyelinating lesions of BCS patients. We evaluated AQP4 expression relative to expression of another astrocytic marker (glial fibrillary acidic protein), the extent of demyelination, lesion staging and perivascular deposition of complement and immunoglobulin in four cases with BCS, and 30 individuals with other neurological diseases. All cases with BCS demonstrated extensive AQP4 loss in both demyelinated and myelinated layers of all actively demyelinating lesions, with perivascular lymphocytic cuffing of T cells, but no deposition of immunoglobulins or complement around vessels. These findings suggest that AQP4 loss occurs in heterogeneous demyelinating conditions, namely NMO and BCS. Furthermore, acute BCS lesions are characterized by extensive AQP4 loss without vasculocentric deposition of complement or immunoglobulin.

Keywords Aquaporin-4 · Astrocyte · Baló's concentric sclerosis · Multiple sclerosis · Neuromyelitis optica

T. Matsuoka · S. O. Suzuki (✉) · T. Iwaki
Department of Neuropathology, Graduate School of Medical Sciences, Kyushu University, 3-1-1 Maidashi, Higashi-ku, Fukuoka 812-8582, Japan
e-mail: sosuzuki@np.med.kyushu-u.ac.jp

T. Matsuoka · J. Kira
Department of Neurology, Graduate School of Medical Sciences, Kyushu University, 3-1-1 Maidashi, Higashi-ku, Fukuoka 812-8582, Japan

T. Tabira
Department of Diagnosis, Prevention and Treatment of Dementia, Graduate School of Juntendo University, 2-11-5 Hongo, Bunkyo-ku, Tokyo 113-0033, Japan

A. T. Ordinario
Department of Neurology and Psychiatry, University of Santo Tomas, Espana Boulevard, Sampaloc, Luzon Manila 1008, Philippines

Introduction

Baló's concentric sclerosis (BCS), a rare variant of multiple sclerosis (MS), was first described by Baló in 1928 [2]. The initial terminology for this entity was encephalitis periaxialis concentrica, which is based on its early definition of "a disease in the course of which the white matter of the brain is destroyed in concentric layers in a manner that leaves the axis cylinders intact" [2]. This condition is relatively frequently reported in some Asian populations including Filipinos [15], southern Han Chinese [38], and Taiwanese [6]. The clinical course is characterized by an acute onset and steady progression to major disability within a few months. It is pathologically characterized by huge, tumor-like brain lesions showing concentric rings of alternating demyelination and preserved myelin layers [7]. Immunohistochemical analysis of ten cases with BCS suggested that this peculiar concentric pattern formation might be attributable to hypoxia-like tissue preconditioning [34]; however, the primary mechanisms that initiate the lesions remain unknown.

On the other hand, neuromyelitis optica (NMO), another demyelinating disorder, also demonstrating extensive lesions in the spinal cord and optic nerves, is thought to be a variant of MS; however, the recent discovery of a specific immunoglobulin G (IgG) against NMO, designated NMO-IgG [20], suggests that NMO is distinct from MS. This IgG targets the aquaporin-4 (AQP4) water channel protein [19], which is strongly expressed on astrocyte foot processes at the blood–brain barrier (BBB) [12]. Autopsied NMO cases show a loss of AQP4 immunostaining in inflammatory lesions, whereas AQP4 expression is increased in the demyelinating plaques in MS patients [27, 30]. The vasculocentric deposition of complement and immunoglobulins in NMO lesions [23] suggests a humoral immune attack against AQP4 on astrocytes, especially as the NMO-IgG/anti-AQP4 antibody is cytotoxic to astrocytes in vitro and in vivo in the presence of complement [3, 4, 13, 14, 31, 32, 36].

Interestingly, Graber et al. [11] recently reported an occurrence of concentric rings of Baló in the brainstem in an Afro-Caribbean patient with NMO. Because AQP4 status has never been studied in BCS, we performed a systematic immunohistological analysis of AQP4 expression in BCS lesions relative to unaffected white matter areas in the same section, astrocyte marker expression, the extent of demyelination, lesion staging and the perivascular deposition of complement and immunoglobulin in four autopsied cases with BCS. All cases showed loss of AQP4 staining but no perivascular deposition of complement or immunoglobulin in the active concentric lesions, suggesting an occurrence of AQP4-related astrocytopathy also in BCS.

Materials and methods

Autopsy cases of BCS and other neurological disorders

This study was performed on archival autopsy brain materials of six concentric demyelinating lesions from four Filipino cases pathologically diagnosed as BCS. The clinical findings of the patients are summarized in Table 1. The cases consisted of two females and two males, and age at autopsy ranged from 23 to 49 years. Disease durations ranged from 0.1 to 0.6 years (median, 0.4 years). In addition, cases with myasthenia gravis (MG) ($n = 2$), spastic paraplegia (SPG) type 2 ($n = 1$), amyotrophic lateral sclerosis (ALS) ($n = 6$), hippocampal sclerosis with temporal lobe epilepsy ($n = 5$), muscular dystrophy ($n = 1$), encephalitis ($n = 3$), including one with anti-*N*-methyl-D-aspartate receptor antibody and another with anti-thyroglobulin antibody, spinocerebellar atrophy (SCA) ($n = 1$), vasculitis ($n = 3$), cerebral infarction ($n = 1$), Pick's disease ($n = 1$), progressive supranuclear palsy ($n = 3$) and multiple system atrophy ($n = 3$) were examined as controls.

Tissue preparation and immunohistochemistry

Autopsy specimens were fixed in 10% buffered formalin and processed into paraffin sections. Sections were routinely stained with hematoxylin and eosin (H&E), Klüver–Barrera (KB) and Bodian or Bielschowsky silver impregnation. The following primary antibodies for immunohistochemistry and staining conditions were used: polyclonal rabbit anti-AQP4 (1:500; Santa Cruz Biotechnology, CA, USA), polyclonal rabbit anti-C3d (1:1000; Dako Cytomation, Glostrup, Denmark), monoclonal mouse anti-C9neo (1:1000; Abcam plc, Cambridge, UK), monoclonal mouse anti-CD68 (1:200; Dako Cytomation, Glostrup, Denmark), monoclonal mouse anti-phosphorylated neurofilament (1:200; Dako Cytomation, Glostrup, Denmark), polyclonal rabbit anti-GFAP (1:1000; Dako Cytomation, Glostrup, Denmark), polyclonal rabbit anti-IgG (1:10000; Dako Cytomation, Glostrup, Denmark), polyclonal rabbit anti-IgM (1:10000; Dako Cytomation, Glostrup, Denmark), monoclonal mouse anti-CD45RO (1:200; Dako Cytomation, Glostrup, Denmark) and monoclonal mouse anti-CD20 (1:200; Dako Cytomation, Glostrup, Denmark). All sections were deparaffinized in xylene and rehydrated in an ethanol gradient. Endogenous peroxidase activity was blocked with 0.3% H_2O_2/methanol. Antigen retrieval was performed by autoclaving sections in 10 mM citrate buffer pH 6.0 before all antibody incubations except for those against AQP4 and GFAP. The sections were then incubated with primary antibody at 4°C overnight. After rinsing, the sections were subjected to either a streptavidin–biotin complex method or an enhanced indirect immunoperoxidase method using Envision (Dako Cytomation, Glostrup, Denmark). Immunoreactivity was detected using 3,3′-diaminobenzidine and sections were counterstained with hematoxylin. Immunohistochemistry for activated complement, immunoglobulins, T cell and B cell markers was performed on randomly selected lesions.

Staging of demyelinating lesions

We classified demyelinating lesions into the following three stages: actively demyelinating lesions, chronic active lesions and chronic inactive lesions based on the density of macrophages phagocytizing myelin debris [16]. Briefly, actively demyelinating lesions were active destructive lesions densely and diffusely infiltrated with macrophages phagocytizing myelin debris, as identified by Luxol fast blue staining. Chronic active lesions were those showing hypercellularity of macrophages restricted to the periphery of the lesions. Chronic inactive lesions were those showing no increase in the numbers of macrophages throughout the

Table 1 Summary of the clinical and pathological findings of cases with Baló's concentric sclerosis

Autopsy	Age (years)	Sex	Disease duration (years)	Relapse rate	Clinically estimated sites of lesions	Pathologically determined sites of lesions
Baló-1	49	M	0.1	NA	Cr (2)[a]	Cr
Baló-2	23	M	0.5	NA	Cr (1)	Cr
Baló-3	28	F	0.3	NA	Cr (1)	Cr
Baló-4	40	F	0.6	NA	Cr (2)	Cr

Cr cerebrum

[a] Number of lesions in parenthesis

lesions. According to the protocol, the six concentric lesions studied were all staged to actively demyelinating lesions.

Comparison of AQP4 expression with myelin loss and astrogliosis

For each lesion, we compared the level of AQP4 expression with the spatial distribution of myelin loss. AQP4 expression levels in region-matched unaffected areas (i.e. gray vs. white mater) in the same section were used as an internal control. To exclude seeming AQP4 down-regulation due to the total loss of astrocytes in such lesions as cavity formation and those totally replaced by macrophages, and to strictly evaluate the AQP4 expression status in the preserved astrocytes in and around the lesions, we confirmed the existence of astrocytes by GFAP staining of neighboring sections for all lesions.

Results

Immunohistochemical findings in control brains

AQP4 expression in pathologically normal brains

AQP4 in normal cerebral tissues from an MG case was diffusely expressed in the cortex, staining the fine processes of the cortical astrocytes (Fig. 1a). Astrocytic perivascular foot processes were more strongly stained with AQP4 than the background neuropil in the cortical gray matter (Fig. 1b, arrows). The glial limiting membranes and subependymal astrocytes also strongly expressed AQP4 (Fig. 1a). There was less AQP4 staining in the white matter than in the cortex, with staining primarily in the perivascular foot processes (Fig. 1c, arrows). In contrast, GFAP immunoreactivity was preferentially observed in the cerebral white matter (Fig. 1d, e). In the cortex, except for the strong staining of the glial limiting membranes (Fig. 1d, arrow), only a few astrocytes were immunopositive for GFAP, with less staining in the perivascular foot processes (Fig. 1f, arrows).

In the cerebellar cortex, both GFAP and AQP4 were expressed in Bergmann glia with radial cytoplasmic processes (Fig. 1g, h), although AQP4 immunoreactivity was generally weaker than that for GFAP. The glial limiting membranes of the cerebellum also strongly expressed GFAP as well as AQP4. In the cerebellar white matter, AQP4 immunoreactivity was mainly observed in the perivascular foot processes, as seen in the cerebral white matter (data not shown).

AQP4 expression in areas of astrogliosis

The normal expression pattern for AQP4 expression was different from that for GFAP as described. However, areas of astrogliosis were generally immunopositive for AQP4 as well as GFAP, in both the gray matter and white matter, regardless of disease types (Fig. 2). For example, hypertrophic gemistocytes in cases of limbic encephalitis (Fig. 2a, b), cerebral infarction (Fig. 2c, d) and SPG type 2 (Fig. 2e, f) showed surface staining for AQP4 in the cytoplasm and processes. Fibrillary gliosis or gliotic scars also showed diffuse AQP4 staining along the glial fibers in cases of SPG type 2 (Fig. 2g, h) and hippocampal sclerosis (data not shown).

Deposition of immunoglobulins and activated complement

Immunohistochemistry for immunoglobulins and activated complement in cerebral tissues from cases with MG, ALS, SCA, vasculitis, limbic encephalitis and cerebral infarction demonstrated weak, diffuse IgG immunoreactivity in the neuronal soma, neuropil, oligodendrocytes, astrocytes, glial limiting membranes and ependymal epithelium, but not in the white matter (data not shown). IgM, C3d and C9neo immunoreactivities were only focally detected in the control cases, and whenever present they were generally confined to blood vessel walls and perivascular regions. Activated complement was not usually co-localized with immunoglobulins; however, in 4 of the 17 cases with non-inflammatory diseases (one each with ALS, SCA, progressive supranuclear palsy and multiple system atrophy) and two of the six cases with inflammatory disorders (anti-*N*-methyl-D-aspartate receptor antibody-seropositive limbic encephalitis and anti-thyroglobulin antibody-seropositive encephalitis), focal perivascular staining for both C3d and IgM was occasionally observed (Fig. 2i, j). In the lesions of patients with ischemic infarction, foamy macrophages were

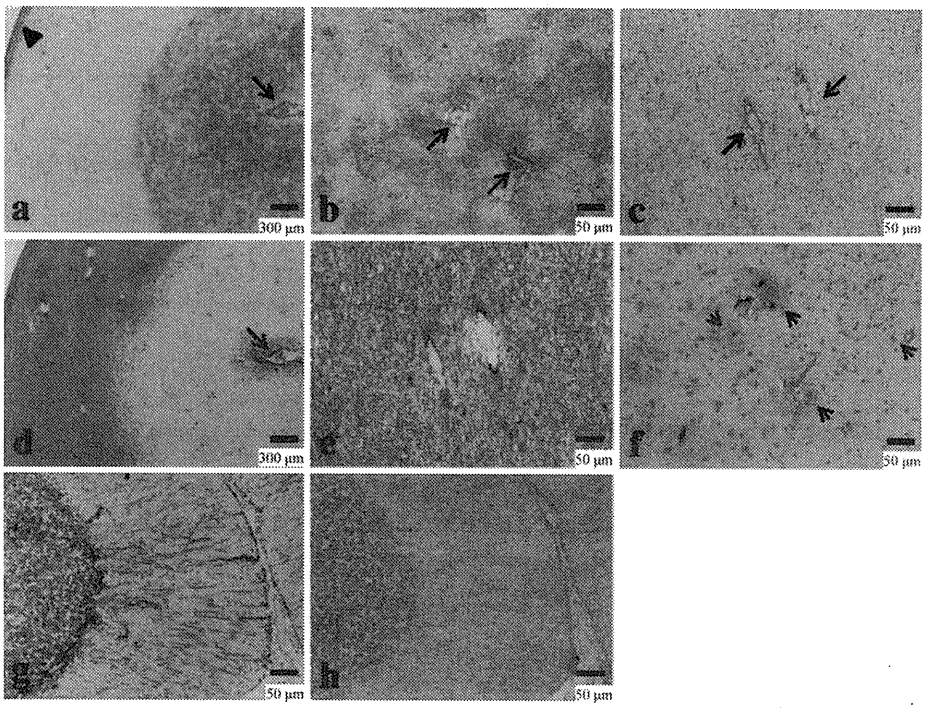

Fig. 1 AQP4 and GFAP expression in normal control brains. A case of MG. AQP4 immunoreactivity is most intense in the glial limiting membrane (*arrow*) and the subependymal astrocytes (*arrowhead*) in the cerebrum. AQP4 is diffusely expressed in the cortex with neuropil staining, while the white matter shows only weak staining (**a**). Higher magnification of the cortex shows strong AQP4 expression in the perivascular foot processes of the cortical astrocytes (*arrows*) (**b**). Higher magnification of the white matter demonstrates an AQP4 staining mainly in the perivascular foot processes of the astrocytes (*arrows*) (**c**). GFAP immunoreactivity is stronger in the white matter than in the cortex. The glial limiting membrane also stains for GFAP (*arrow*) (**d**). Higher magnification of the white matter shows strong GFAP immunoreactivity (**e**). Higher magnification of the cortex shows only scattered GFAP immunoreactive cortical astrocytes and faint staining in the vascular foot processes of astrocytes (*arrows*) (**f**). In the cerebellar cortex, GFAP stains Bergmann glia with radial cytoplasmic processes (**g**). In the cerebellar cortex, AQP4 immunoreactivity is observed in Bergmann glia with radial cytoplasmic processes (**h**). AQP4 (**a–c**, **h**) and GFAP (**d–g**) immunohistochemistry. *Scale bar* 300 μm (**a**, **d**), 50 μm (**b**, **c**, **e–h**), *AQP4* aquaporin-4, *GFAP* glial fibrillary acidic protein, *MG* myasthenia gravis

commonly stained for C3d, C9neo, IgM and IgG. In addition, surface staining of reactive astrocytes was seen with IgG immunostaining, probably due to diffusion of the serum in the affected brain tissue (Fig. 2k–n).

Immunohistochemical findings in BCS

All cases with BCS showed concentric rings of alternating demyelination and preserved myelin layers in the cerebral white matter (Fig. 3a, d). The lesion center was entirely covered with GFAP immunostaining. In the centers of all six actively demyelinating lesions, AQP4 staining was markedly diminished, despite the strong GFAP immunoreactivity (Table 2, Fig. 3c, f, g–l) in both gemistocytic astrocytes (Fig. 3h, i) and astrocytic vascular foot processes (Fig. 3k, l) compared with the unaffected white matter regions with preserved myelin staining (Fig. 3j). The myelin staining negative, peripheral layers of the lesions showed marked decreases of both GFAP and AQP4 staining. High-power field inspection revealed that these areas were almost totally replaced by foamy macrophages (Fig. 3m), with only a small number of highly degenerated GFAP-positive astrocytic processes (Fig. 3n) and axon fragments positive for silver staining (Fig. 3o) and phosphorylated neurofilaments (Fig. 3p). Despite the existence of a few GFAP-positive structures, these areas were totally devoid of AQP4 staining (Fig. 3q). In all lesions, perivascular cuffing with lymphocytes was observed (Fig. 3r). There was dense infiltration of foamy macrophages including myelin debris in the demyelinating layers (Fig. 3s). The perivascular infiltrates predominantly consisted of T cells, while vasculocentric deposition of immunoglobulins (IgG and IgM) or activated complement (C3d and C9neo) was never observed in any of the lesions examined (Table 2; Fig. 3t–v).

Discussion

We performed an immunohistopathological study on AQP4 expression in autopsy cases of BCS. Surprisingly, all cases

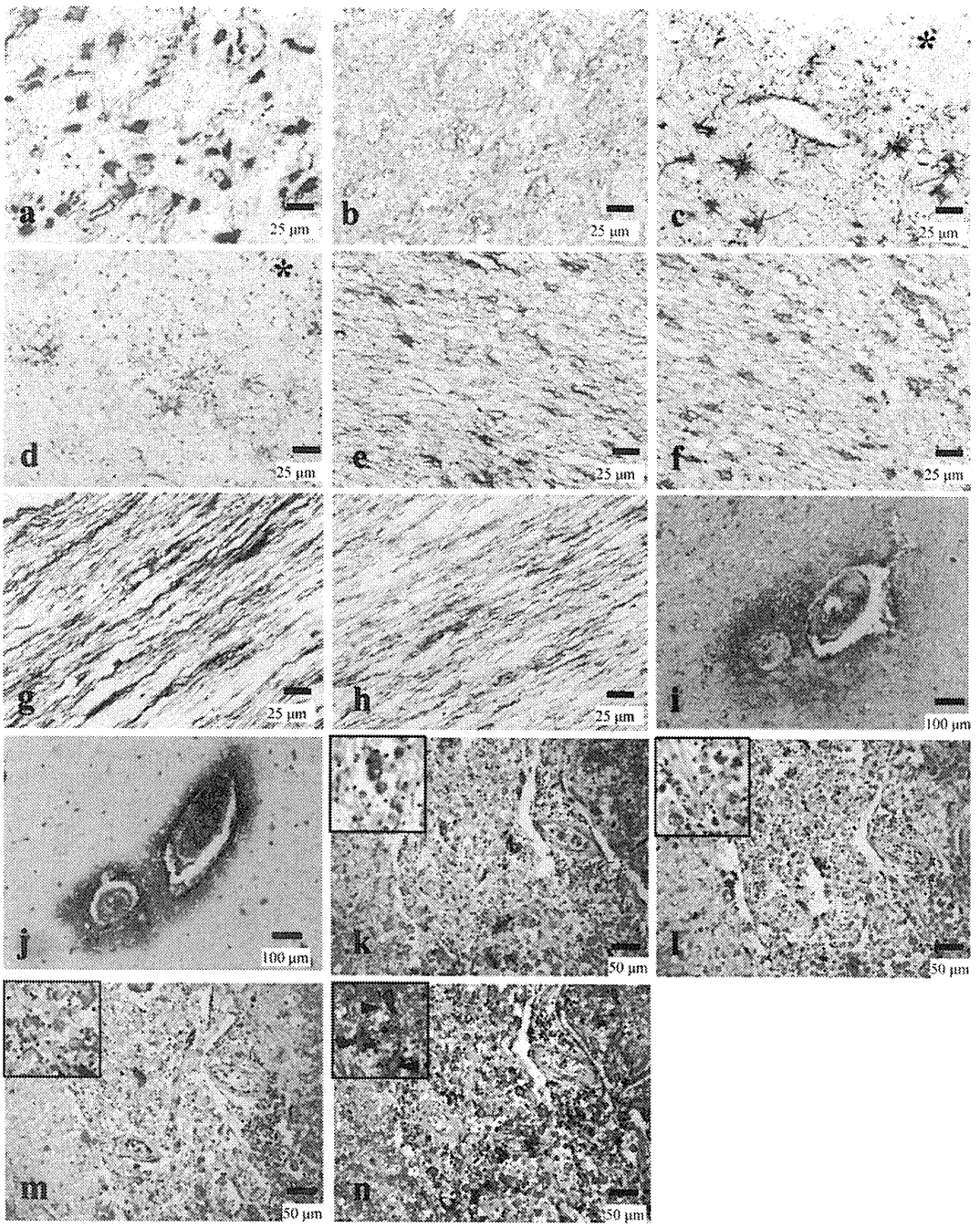

Fig. 2 AQP4, immunoglobulin and complement expression patterns in cases with other neurological diseases. (**a–h**) AQP4 expression in astrogliosis. GFAP-positive gemistocytes (**a**, **c**, **e**) show membranous staining for AQP4 (**b**, **d**, **f**) in cases of limbic encephalitis (**a**, **b**), cerebral infarction (**c**, **d**) and SPG type 2 (**e**, **f**). *Asterisks* in **c** and **d** indicate necrotic areas. Fibrillary gliosis seen in the corpus callosum of the same SPG type 2 case is positive for both GFAP (**g**) and AQP4 (**h**). **i–n** Deposition of immunoglobulins and activated complement (C3d and C9neo) in cases with other neurological diseases. Serial sections distant from focal lesions in the pons from a case with SCA. C3d staining is detected in the perivascular areas (**i**). IgM staining shows a similar pattern to C3d staining (**j**). (**k–n**) Serial sections of the cerebral tissues from a case with cerebral infarction. Numerous macrophages filled with C3d-positive granules in the lesions (*inset* macrophages) (**k**). C9neo staining shows a similar pattern to C3d staining (*inset* macrophages) (**l**). IgM staining shows a similar pattern to activated complement staining (*inset* macrophages) (**m**). IgG staining shows the similar pattern as IgM staining. In addition, staining outlining the cytoplasm of hypertrophic astrocytes was noted (*inset arrowheads*) (**n**). GFAP (**a**, **c**, **e**, **g**), AQP4 (**b**, **d**, **f**, **h**), C3d (**i**, **k**), IgM (**j**, **m**), C9neo (**l**) and IgG (**n**) immunohistochemistry. *Scale bar* 100 μm (**i**, **j**), 50 μm (**k–n**), 25 μm (**a–h**), *AQP4* aquaporin-4, *GFAP* glial fibrillary acidic protein, *SPG* spastic paraplegia, *SCA* spinocerebellar atrophy

with BCS uniformly demonstrated extensive AQP4 loss in all actively demyelinating lesions with perivascular lymphocytic cuffing, but no deposition of immunoglobulins or complement around the blood vessels. Our study indicates that AQP4 loss could occur not only in NMO but also in BCS lesions.

We found a similar AQP4 expression pattern in normal brain tissues to what has been previously reported [27, 30], although we used a different anti-AQP4 antibody to the ones used in those studies. For example, normal cortical astrocytes were diffusely immunostained for AQP4 and weakly immunostained for GFAP, whereas white matter astrocytes showed a reverse pattern. AQP4 is strongly expressed in the glial limiting membranes, and subependymal and perivascular astrocytes. In control diseased brains, both reactive, gemistocytic astrocytes and areas of chronic fibrillary gliosis showed high levels of AQP4 expression regardless of the cause, as previously reported [1, 18, 27, 30]; however, since all the BCS lesions examined in this study were acute lesions, we did not observe chronic fibrillary gliosis and resultant upregulation of AQP4. On the other hand, demyelinating lesions with AQP4 loss generally showed numerous GFAP-immunopositive, gemistocytic astrocytes. In addition, AQP4 expression was lost from GFAP-positive perivascular foot processes. Although some of the myelin-negative foci at the periphery of the concentric lesions showed a decrease in both GFAP and AQP-4 staining, these areas were proven to be necrotic foci with only a small amount of debris from astrocytic processes and axons. Therefore, acute BCS lesions are characterized by AQP4 loss in GFAP-expressing astrocytes and their vascular foot processes, distinct from the staining pattern in NMO in which astrocytes reportedly lose both GFAP and AQP4 staining [27].

This is the first report to show AQP4 loss in BCS cases, not only in the layers showing demyelination, but also in the layers with preserved myelin. All actively demyelinating lesions in BCS showed the same pattern of AQP4 loss, but other acute inflammatory conditions such as limbic encephalitis did not show such AQP4 loss in lesions, suggesting that AQP4 loss is an inherent component of this acute disease. We are currently examining AQP4 status in NMO and MS cases in comparison with that in BCS cases.

All autopsied materials were archival ones taken long before the discovery of NMO-IgG/anti-AQP4 antibody, and the anti-AQP4 antibody statuses of the present BCS cases are unknown. However, because the vasculocentric deposition of complement and immunoglobulins was not confirmed in any of the BCS lesions, an autoantibody and complement-mediated mechanism, which is considered to be unique to NMO, may not be operative in BCS. In future, it will be necessary to measure levels of anti-AQP4 antibody in a large clinical series of BCS patients.

Fig. 3 Representative AQP4 expression pattern in concentric or lamellar demyelinating lesions. Serial sections of the cerebral tissue with actively demyelinating lesions in the white matter from case Baló-1 (**a–c**) and case Baló-2 (**d–s**). The cerebral white matter reveals concentric or lamellar demyelinated lesions (**a**, **d**). GFAP is expressed in the lesion centre, but is largely diminished in the lamellar necrotic foci at the lesion edge (*arrows*) (**a**, **b**, **d**, **e**). AQP4 immunoreactivity is largely lost in the lesion centre with lamellar myelin-staining patterns (**c**, **f**). Numerous reactive, hypertrophic astrocytes are seen in both the demyelinating and preserved myelin layers (**g**). Astrocytes in (**g**) strongly express GFAP (**h**) but lack surface staining for AQP4 (**i**). In the unaffected white matter with preserved myelin staining and no inflammatory infiltration in the same section (the area indicated by *arrowhead* in **d**), non-reactive astrocytes show AQP4 staining on the cell surface and their processes (**j**) and AQP4 expression is also preserved in the perivascular astrocytic foot processes (**k**). In the lesions, however, the perivascular AQP4 staining also disappears (**l**). High-power field views of GFAP-negative necrotic foci at the lesion edge (indicated by *arrows* in **a**, **b**, **d**, **e**) reveal dense infiltration of foamy macrophages (**m**), a small number of highly degenerative, remaining astrocytes (**n**), axons (*arrowheads* in **o**, **p**) and foamy spheroids (*arrows* in **p**). AQP4 immunoreactivity is totally lost in the necrotic areas (**q**). Perivascular accumulation of lymphocytes is noted all over the lesion (**r**). Dense infiltration of foamy macrophages phagocytosing myelin debris in the demyelinating layer (**s**). Perivascular lymphocytes are immunopositive for the T cell marker CD45RO (**t**), but negative for the B cell marker CD20 (**u**). IgG, IgM, C3 and C9neo labeling is detected in some glial cells, but not in the perivascular areas (**v**). Klüver–Barrera staining (**a**, **d**, **s**), hematoxylin and eosin staining (**g**, **m**, **r**), GFAP (**b**, **e**, **h**, **n**) AQP4 (**c**, **f**, **i–l**, **q**), Bielschowsky's silver staining (**o**), phosphorylated neurofilament (**p**), CD45RO (**t**), CD20 (**u**) and IgG, IgM, C3 and C9neo (**v**) immunohistochemistry. *Scale bar* 4 mm (**a–f**), 100 μm (**v**), 50 μm (**k**, **l**, **t**, **u**), 25 μm (**g–j**, **m–s**). *AQP4* aquaporin-4, *GFAP* glial fibrillary acidic protein

The lesions in BCS are classified as type 3 lesions as described by Lucchinetti et al. [22], and the disease is considered to be an oligodendrocytopathy. However, we found AQP4 down-regulation in both demyelinated and myelinated layers, suggesting that astroglial damage occurs more widely than oligodendroglial damage. Hypoxia-like tissue injury may contribute to Baló's lesions [24, 34], which can show restricted diffusion on diffusion-weighted MRI sequences, as happens in acute stroke [39]. Because AQP4 is down-regulated in hypoxic conditions and in the ischemic core at the acute stage [9, 10, 17, 26], vessel obliteration or mitochondrial impairment [24] associated with heavy lymphocytic inflammation may lead to tissue hypoxia and AQP4 down-modulation in BCS.

It has recently been reported that reactive astrocytes that form perivascular scars act as barriers to leukocytes and that conditioned ablation of reactive astrocytes strengthens inflammation [37]. Because AQP4 deletion impairs glial scar formation [35], down-regulation of AQP4 in BCS may enhance inflammatory changes through interruption of perivascular glial scar formation. On the other hand, AQP4 knockout mice show reduced cytotoxic edema following tissue ischemia and hypoxia [25], suggesting that AQP4 down-regulation is protective. Similarly, experimental

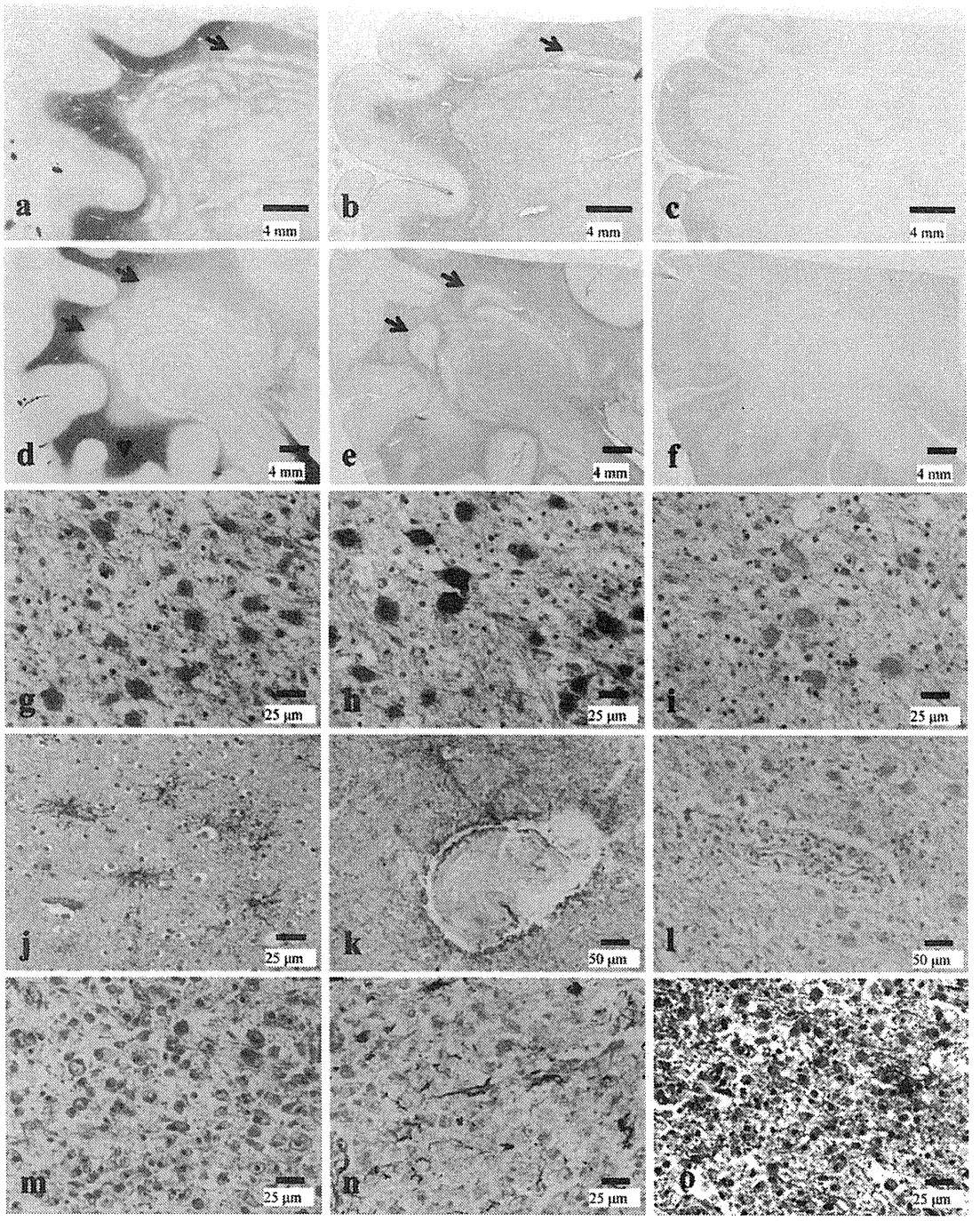

autoimmune encephalomyelitis induced by myelin oligodendrocyte glycoprotein peptide is attenuated in AQP4 knockout mice [21]. These observations suggest that AQP4 down-modulation could be neuroprotective in hypoxia-induced cytotoxic edema as well as in inflammatory demyelinating lesions, which may also be applicable to BCS. On the other hand, it has been reported that AQP4 inhibition causes exacerbation of vasogenic edema [29]. The formation of tumor-like, highly edematous BCS lesions thus might mainly result from vasogenic edema.

In MS, AQP4 loss in actively demyelinating lesions has so far not been reported; Misu et al. [27] found no loss or exaggerated expression of AQP4 in MS plaques, while Roemer et al. [30] detected AQP4 loss in the chronic inactive lesions, suggesting that stage-dependent loss of AQP4 may occur in some MS lesions. Therefore, extensive

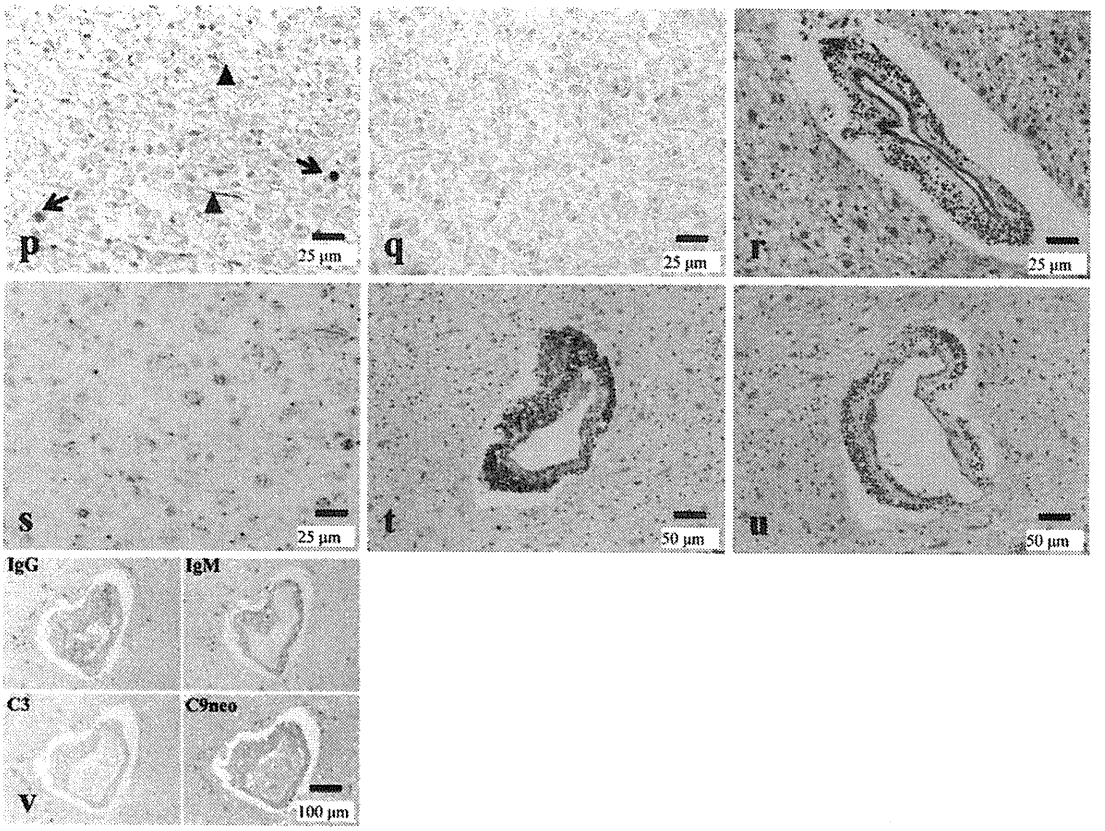

Fig. 3 continued

Table 2 Summary of the pathological findings in demyelinating lesions in cases with Baló's concentric sclerosis

Case	Lesion	Stage	AQP4 loss	T cell infiltration	Perivascular deposition of immunoglobulins and complement
Baló-1	Cr1	Active	Extensive	Perivascular	No
	Cr2	Active	Extensive	Perivascular	No
Baló-2	Cr1	Active	Extensive	Perivascular	No
Baló-3	Cr1	Active	Extensive	Perivascular	No
Baló-4	Cr1	Active	Extensive	Perivascular	No
	Cr2	Active	Extensive	Perivascular	No

AQP4 aquaporin-4, *Cr* cerebrum

AQP4 loss in the acute lesions without vasculocentric deposition of complement or immunoglobulin is considered to be characteristic of BCS.

There are several lines of experimental evidence that anti-AQP4 antibody-independent impairment of astrocytes causes AQP4 loss followed by demyelination. Sharma et al. [33] reported lipopolysaccharide-induced demyelinating lesions in rats showed loss of AQP4 and retraction of astrocytic vascular foot processes. Likewise, Wolburg-Buchholz et al. [40] demonstrated that ultrastructural distribution of AQP4 is altered in the astrocytic foot processes followed by destruction of the BBB in a murine experimental autoimmune encephalomyelitis model immunized with proteolipid protein peptide. Indeed, the astrocytes in the active lesions in our BCS cases showed extremely hypertrophic, abnormal reacting morphology suggestive of considerable functional impairment including loss of AQP4 expression. The mechanism underlying such anti-AQP4 antibody-independent AQP4 loss is currently unknown. However, phosphorylation-related internalization of AQP4 resulting from a variety of stimuli might initiate this process [5, 8, 28].

Future studies on astrocytopathy as well as the dynamic plasticity of astrocytes may shed light on the mechanisms underlying the alternating myelinated and demyelinated lesions observed in BCS.